EARTH SCIENCES
RESEARCH JOURNAL
Earth Sci. Res. J. Vol. 29, No. 2 (June, 2025): 149 - 167

UNIVERSIDAD NACIONAL DE COLOMBIA

GEOLOGY

Clastic Source and Depositional Environment of Mixed Carbonate-Clastic Sequences in the Oligocene Nari Formation from the Hundi Anticline, Karachi Embayment, Indus Basin, Pakistan

Surriya Bibi Ahmedani[1,2], Asghar A. A. D. Hakro[1], Abdul Shakoor Mastoi[1], Aijaz Ali Halepoto[1]*, Ali Ghulam Sahito[1], Shamim Akhtar[3], Rafique Ahmed Lashari[1]
1 Centre for Pure and Applied Geology, Faculty of Natural Sciences, University of Sindh, Jamshoro, Pakistan
2 Government Zubeda Girl College Hyderabad, College Education Department, Government of Sindh
3 Department of Earth Sciences, University of Sargodha, Punjab, Pakistan
*Corresponding Author Email: aijaz.halepoto@usindh.edu.pk

ABSTRACT

The Oligocene Nari Formation in the Karachi Embayment of the Indus Basin, Pakistan, consists of interbedded limestone, sandstone and shale. This study aims to elucidate the source of clastic rocks and depositional environment of these mixed carbonate-clastic successions using integrated outcrop observations, facies analysis and petrography. Outcrop-based facies analysis identified six facies; including arenaceous limestone, calcareous sandstone, argillaceous sandstone, laterite/oxidized sandstone, arenaceous shale and calcareous mudstone. Petrographic analysis further distinguished five limestone-dominated microfacies and two sandstone-dominated petrofacies. The microfacies are dominated by packed and sparse biomicrites composed primarily of calcite, with minor contribution from terrigenous minerals. The petrofacies include sub-arkose and quartz arenite, which are predominantly composed of quartz, with lesser proportion of feldspar, clay minerals and other minerals. The mineral composition of the petrofacies suggest a granitic source, likely derived from the Indian Craton to the east. Facies analysis suggests that the Nari Formation was deposited in a range of environments from outer ramp to fluvio-deltaic settings. The overall facies succession reflects a progradational trend, interpreted as a response to regional regression during the Himalayan orogeny. This study will bring new perspectives to refine the interpretations of sedimentary processes in mixed carbonate-clastic environments in the region thereby advancing our understanding to geological history of the study area.

Keywords: Clastic Source, Depositional Environment, Mixed Carbonate-Clastic rocks, Petrography, Oligocene, Nari Formation

Fuente clástica y entorno deposicional de secuencias mixtas carbonato-clásticas en la Formación Nari del Oligoceno del anticlinal Hundi, ensenada de Karachi, cuenca del Indo, Pakistán

RESUMEN

La Formación Nari del Oligoceno, en la ensenada Karachi de la cuenca del Indo (Pakistán), está compuesta por intercalaciones de caliza, arenisca y lutita. Este estudio busca dilucidar el origen de las rocas clásticas y el entorno deposicional de estas sucesiones mixtas carbonato-clásticas mediante observaciones integradas de afloramientos, análisis de facies y petrografía. El análisis de facies basado en afloramientos identificó seis facies: caliza arenisca, arenisca calcárea, arenisca arcillosa, arenisca laterítica/oxidada, lutita arenisca y lutita calcárea. El análisis petrográfico distinguió además cinco microfacies con predominio de caliza y dos petrofacies con predominio de arenisca. Las microfacies están dominadas por biomicritas compactas y dispersas, compuestas principalmente de calcita, con una contribución menor de minerales terrígenos. Las petrofacies incluyen arenita subarcosa y cuarzo, compuestas predominantemente de cuarzo, con una menor proporción de feldespato, minerales arcillosos y otros minerales. La composición mineral de las petrofacies sugiere una fuente granítica, probablemente al este del Cratón Indio. El análisis de facies sugiere que la Formación Nari se depositó en diversos ambientes, desde la rampa exterior hasta entornos fluviodeltaicos. La sucesión general de facies refleja una tendencia progradacional, interpretada como una respuesta a la regresión regional durante la orogenia del Himalaya. Este estudio aporta nuevas perspectivas para refinar la interpretación de los procesos sedimentarios en ambientes mixtos carbonato-clásticos en la región, lo que contribuye a la comprensión de la historia geológica del área de estudio.

Palabras clave: Fuente clástica, entorno deposicional, rocas carbonatadas-clásticas mixtas, petrografía, Oligoceno, Formación Nari

Record
Manuscript received: 03/08/2024
Accepted for publication: 14/05/2025

How to cite this item:
Ahmedani, S. B., Hakro, A. A., Mastoi, A. S., Halepoto, A. A., Sahito, A. G., Akhtar, S., Lashari, R. A. (2025). Clastic Source and Depositional Environment of Mixed Carbonate-Clastic Sequences in the Oligocene Nari Formation from the Hundi Anticline, Karachi Embayment, Indus Basin, Pakistan. *Earth Sciences Research Journal, 29*(2), 149-167. https://doi.org/10.15446/esrj.v29n2.116089

ISSN 1794-6190 e-ISSN 2339-3459
https://doi.org/10.15446/esrj.v29n2.116089

1. Introduction

Mixed carbonate and clastic deposits provide an important record of tectonic, depositional and paleogeographic changes (Zuffa 1980; Doyle & Roberts 1988; Zohdi et al. 2013; Brandano & Ronca 2014; Anan 2014; Nikbakht et al., 2019; Zecchin et al. 2021; Tong et al. 2023; Zuchuat et al. 2023; Robles-Salcedo & Vicedo 2023; Hussein et al. 2024; Jamrich et al. 2024). The changes from carbonate to clastic deposition and viceversa are determined by tectonic setting, climatic fluctuations and changes in sea level (Zuffa 1980; Mount 1985; Doyle & Roberts 1988; Nichols 2009; Zeller et al. 2015; Zecchin et al. 2021; Shehata et al. 2021; Zecchin et al. 2023; Della Porta et al. 2023; Hussein et al. 2024; Gil-Gil et al. 2024). Oligocene is a significant epoch in the tectonic history of the Indus Basin, characterized by early stage of continent-continent collision, dynamic basin geometry, retreating sea-level and frequently variable depositional conditions (Raza et al. 1990; Bender & Raza 1995; Smewing et al. 2002b; Ghani et al. 2023; Ahmedani et al. 2024a). The Nari Formation of The Oligocene age stands out as a key stratigraphic unit, which offers valuable insights into the relationship of clastic and carbonate sedimentation during this time (Ahmedani et al. 2024b). Therefore, clastic source and depositional environment of mixed carbonate-clastic successions within the Nari Formation, deposited in a dynamic basin conditions provide invaluable constraints regarding the tectonic-sedimentary processes. Furthermore, better understanding towards the facies variations and sedimentary processes in mixed carbonate-clastic sequences is crucial for the reservoir characterization, because such units often serve as important hydrocarbons as well as groundwater reservoirs.

The Nari Formation of the Oligocene age is one of the most important mixed carbonate-clastic sequence, exposed in the Karachi Embayment, Indus Basin, Pakistan. The term "Nari series" was coined by Blanford (1876) for Oligocene sequence of Indus Basin, after the "Nari River" in the Kirthar Range, Indus Basin, Pakistan. Subsequently, Blanford (1879) separated Oligocene rocks into "Lower Nari Series" and "Upper Nari Series". Williams (1959) used the term "Nari Formation" for the "Nari Series". "Lower Nari Series" of Blanford (1879) was named "Nal Limestone" by Hunting Survey Corporation (1960) and "Nal member" (Cheema et al., 1977). They proposed "Momani Group" to include the Nari Formation and overlying Gaj Formation of Miocene age. Nari Formation has been studied in terms of echinoids fossil assemblages (Duncan & Sladen, 1884; Hunting Survey Carporation, 1960; Khan, 1968), reservoir potential (Mahmud & Sheikh, 2009), grain size analysis and depositional environment (Khokhar et al., 2016; Hakro et al., 2021; Samtio et al., 2021; Ahmedani et al. 2024b), provenance (Ahmed et al., 2020; Hakro et al., 2022), petrophysics (Shar et al., 2021a), geochemistry (Shar et al., 2021b) and diagenesis (Ahmedani et al., 2024a). However, high-resolution facies analysis of the Nari Formation to understand its clastic source, depositional environment and construct a systematic sequence of depositional events is not yet attempted. The paleogeographic and tectonic conditions, which governed the deposition of mixed carbonate-clastic sequences of the Nari Formation, remained largely unexplored. This research is focused on thorough and in-depth facies investigation of the Nari Formation to unravel the clastic source and depositional environment. This study aimed to contextualize these findings in the broader regional tectonic framework.

2. Geological Setting

The Indus Basin was located on the northwestern passive margin of the Indian Plate (Kadri 1995; Siddiqui 2016; Rizwan et al. 2020; Bilal et al. 2023b). It The Indus Basin consists of a very thick Precambrian to Recent sedimentary record with marked absence of the Ordovician to Carboniferous record (Kazmi & Jan 1997; Kazmi & Abbasi 2008; Shah 2009). Terrigenous clasts to the Indus Basin were supplied by the Indian Craton located on its eastern boundary of the Indus Basin (Bender & Raza 1995; Khan et al. 2002; Hakro et al. 2018; Qasim et al. 2022; Sarwar et al. 2024). The Indus Basin experienced extensional tectonics during the Middle Jurassic to Late Cretaceous, when the Indian Plate rifted off from the western Gondwanaland fragments (Powell et al. 1988; Besse & Courtillot 1988; Ahmed et al. 2018; Halepoto et al. 2025). Mesozoic extensional tectonics controlled the basin geometry and sedimentation pattern of younger rocks (Kadri 1995; Hedley et al. 2001; Smewing et al. 2002a; Ahmed et al. 2018; Halepoto et al. 2025). Sedimentary rocks of the Indus Basin were intensely deformed during the collision of the Indian Plate with the Eurasian Plate since the Late Paleocene / Early Eocene (Allemann 1979; Bannert et al. 1992; Fowler et al. 2004; Jadoon et al. 2020; Ghani et al. 2023). The early stage of deformation of the northwestern margin of the Indian Plate during the Oligocene had profound control on the depositional environment in the Indus Basin, Pakistan. The marine conditions in the Indus Basin started to retreat during the Late Eocene and Early Oligocene. Major part of the Indus Basin uplifted during the Oligocene, which is marked by either absence of the Oligocene sequence or fluvial rocks (Raza et al., 1990). Constantly retreating sea occupied position of the Karachi Embayment during the Oligocene (Raza et al., 1990; Cheema et al., 2009). The Karachi Embayment is located in southern extreme of the Indus Basin (Figure 1), which developed due to its abrupt down-warping outer shelf of the Indus Basin during Mesozoic rifting (Zuberi & Dubois, 1962). This Embayment is unique tectonic element as it contains conformable K/T (Cretaceous / Tertiary) boundary, thickest Paleocene strata of the Indus Basin and last phases of marine sedimentation up to Miocene-Early Pliocene (Meissner & Rehman 1973; Raza et al. 1990; Bender & Raza 1995; Kadri 1995). Mostly the Karachi Embayment contains exposures of Eocene and younger strata, which are folded in NS trending en echelon anticlines. The exposures of Oligocene strata in the Karachi Embayment may provide a detailed record about the sediment source and depositional environment during this epoch. The stratigraphy and tectonics of the Indus Basin is well documented by Williams (1959), Hunting Survey Corporation (1960), Zuberi & Dubois (1962), Kazmi & Rana (1982), Raza et al. (1990), Bender & Raza (1995), Kadri (1995), Kazmi & Jan (1997), Kazmi & Abbasi (2008), Shah (2009) and Siddiqui (2016), which is summarized in Figure 2.

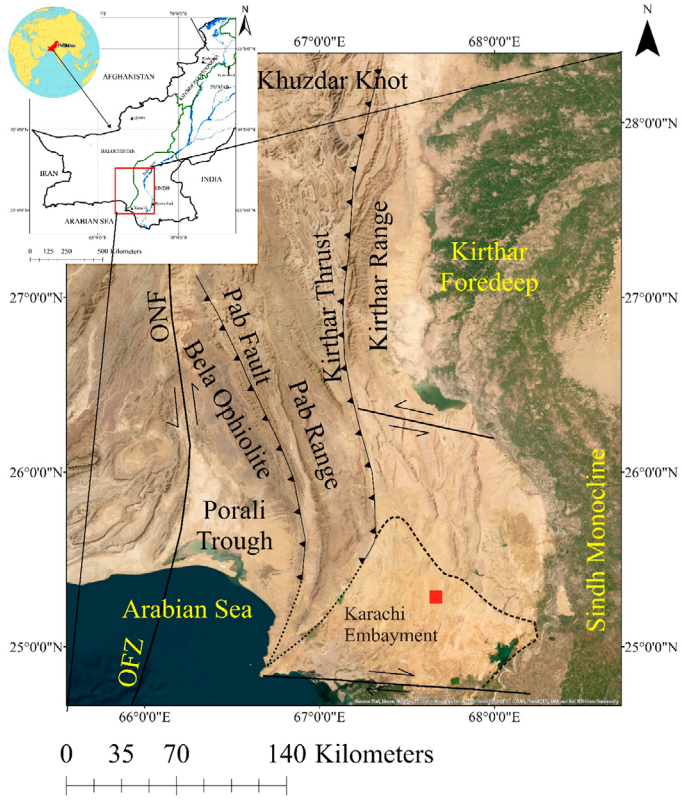

Figure 1. Satellite image of part of southern Pakistan, showing tectonic elements and location of Hundi anticline in red rectangle within Karachi Embayment modified after; Hunting Survey Corporation, 1960; Zuberi & Dubois, 1962; G. Sarwar & De Jong, 1979; Kazmi & Rana, 1982; Bannert et al., 1992; Halepoto et al., 2022. (Image Source: Esri, Maxar, GeoEye, Earthstar Geographics, CNES/ Airbus DS, USDA, USGS, AeroGRID, IGN, and the GIS User Community).

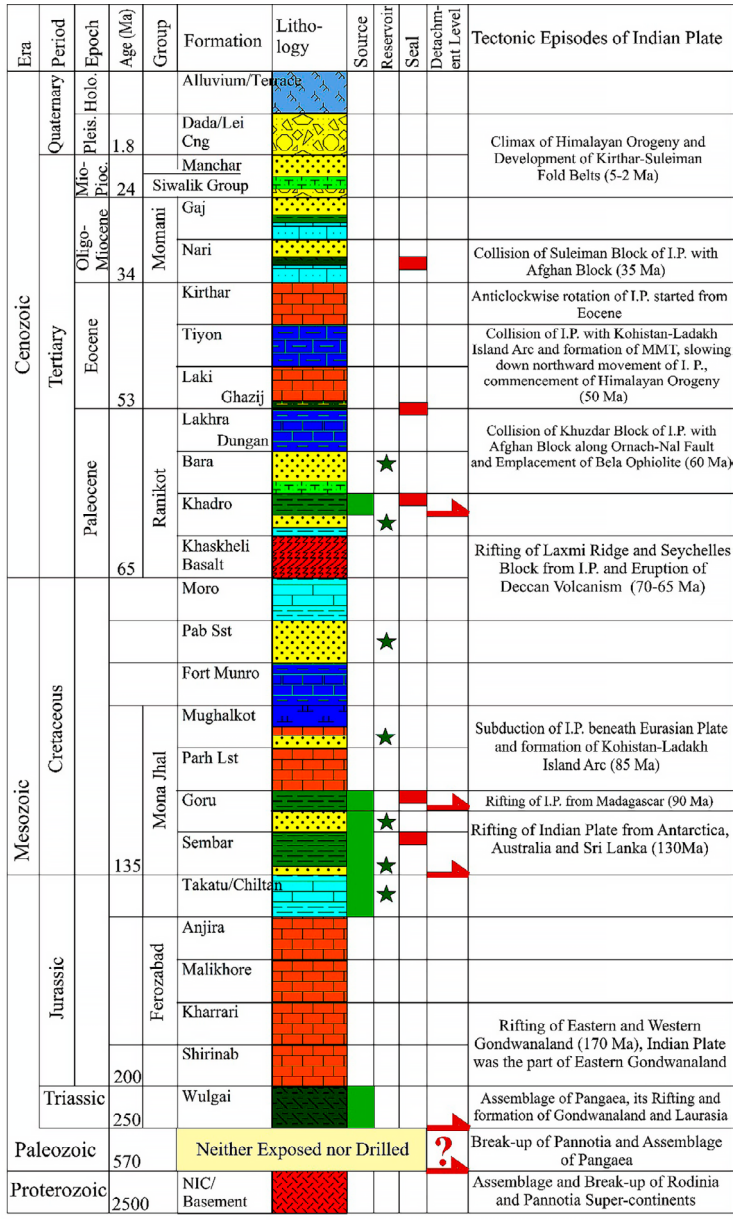

Figure 2. Stratigraphy of the Southern Indus Basin and important tectonic episodes of the northwestern margin of the Indian Plate (I.P.) After; Hunting Survey Corporation, 1960; Burret, 1974; Powell, 1979; Allemann, 1979; Barron & Harrison, 1980; Devey & Lightfoot, 1986; Coward et al., 1988; Raza et al., 1990; Jadoon et al., 1992; Kadri, 1995; Bender & Raza, 1995; Unrug, 1997; Kazmi & Jan, 1997; Mcloughlin, 2001; Shah, 2009; Siddiqui, 2016; Hinsch et al., 2018; Ahmed et al., 2018; Jadoon et al., 2021; Halepoto et al., 2025.

3. Methodology

The well exposed and 130 m thick section of Nari Formation was measured from the eastern flank of Hundi anticline (Lat. 25º, 16' N, Long. 67º, 41' E), Karachi Embayment, Pakistan (Figures 1, 3), through Jaccob's staff and tape_brunton methods (Compton, 1962; Coe et al. 2010). The identified limestone and shale facies were described after Wilson (1975) and Pettijohn (1975) respectively, whereas, sandstone facies were described after Pettijohn (1975) and Pettijohn et al. (1987). Thirty two rock samples, one from each strata, were collected for detailed description and petrographic analysis (Figure 4). The samples were sorted in different lithological groups based on their macroscopic features such as texture, compaction etc. Eleven thin sections from hard and compact samples were prepared to investigate their texture, mineral composition microfacies and petrofacies. The petrographic analysis was carried out under "Leica DM 2500P Polarizing Microscope" at "Advanced Research Laboratories, Centre for Pure and Applied Geology, University of Sindh, Jamshoro, Pakistan". The sections were point-counted using Gazzi-Dickinson point-counting method to calculate the percentage of textural and mineralogical attributes (Ingersoll et al., 1984). The clastic source and tectonic setting of the sandstone was interpreted using ternary diagram (Dickinson et al., 1983) by considering QFL (Quartz, Feldspar, Lithics) fraction as 100%. The sandstone petrofacies were named based on their framework composition after Mcbride (1963). Due to the mixed nature, microfacies are classified according to the classification scheme proposed by Mount (1985). The identified microfacies were compared with the standard microfacies proposed by Wilson (1975) and Flugel (2004) to validate their environmental interpretation. The field and petrographic data were integrated to discuss the depositional environment of the Nari Formation in study area. Different softwares, such as ArcGIS, Rockware LogPlot and Corel Draw etc., were also used to prepare maps, logs and pictures of present work.

4. Facies Analysis

In the study area, the Nari Formation has a conformable lower contact with the Late Eocene Kirthar Formation, while its upper contact is unconformably overlain by Holocene alluvium (Figures 3, 5a). The formation exhibits significant vertical variations in lithology. Based on field observations, six distinct facies, comprising limestone, sandstone and shale, have been identified. Limestone facies dominate the lower part, whereas sandstone facies are more prominent in the upper part of the Nari Formation (Table 1).

4.1 Arenaceous Limestone Facies (LF-1)

Description: These are the most dominant facies, constituting more than half of the Nari Formation in the studied section. They comprise nineteen strata grouped into eight intervals, with a total thickness of 83 meters out of the 130 meters recorded (Figure 4). These facies has maximum thickness of about 75 meters within the lower 90 meters of the formation. The thickness of these facies decrease from bottom to top and are gradually replaced by calcareous and argillaceous sandstone towards top of the formation. The lower strata of these facies are rich in mega and microfossils. These facies occur in different colors such as light-brown, yellowish-brown, reddish-brown, reddish-yellow and orange-yellow and is well compact and thin to thick-bedded (Figure 5b-d).

Interpretation: The lithological features suggest deposition on a shallow marine platform with minor clastic influx from surrounding landmass. The abundance of fossils indicate a stable, nutrient-rich, shallow marine ecosystem conducive for growth and preservation of marine life (Selley 2000; Saker-Clark 2019; Haqbin et al. 2024). The color variations likely reflect changes in water chemistry, oxidation conditions and organic matter content, influenced by local environmental fluctuations during deposition (Aguilera-Franco & Romano, 2004; Boggs, 2009).

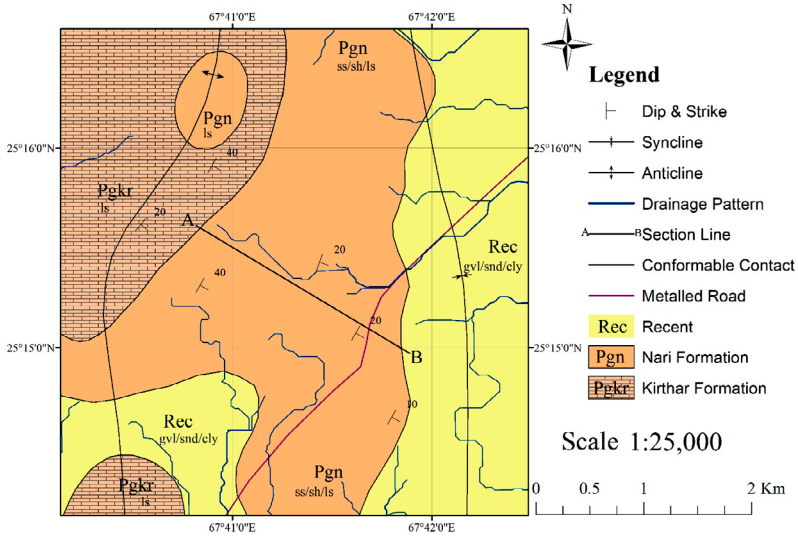

Figure 3. Geological map of the study area, where AB line indicates the measured stratigraphic section during present study (modified after Hunting Survey Corporation, 1960).

Table 1. Summarized characteristics of individual facies and their interpreted depositional environments.

Facies Code	Facies Name	Thickness (m)	Lithology	Color(s)	Sedimentary Structures	Interpretation
LF-1	Arenaceous Limestone	83	Fossiliferous, compact limestone	Light to reddish/ yellowish brown	Thin to thick bedding	Shallow marine platform, low clastic influx
LF-2	Calcareous-Gypsiferous Mudstone	2	Soft mudstone with gypsum, calcite	Yellowish grey to light brown	Sharp, erosional base	Evaporative lagoon in arid/semi-arid conditions
LF-3	Calcareous Sandstone	17	Fine to medium sandstone, calcareous	Brown, grey	Thin-thick bedding	Fluctuating transitional to shallow marine conditions
LF-4	Laterite/Oxidized Sandstone	5	Iron-rich, oxidized sandstone	Reddish brown	Thick bedding	Tropical weathering, sub-aerial exposure
LF-5	Arenaceous Shale	8	Silty shale, fissile, nodular	Light grey/yellow	Fissility, erosional base	Fluvial to transitional, periodic flooding
LF-6	Argillaceous Sandstone	15	Sandstone with mud matrix	Reddish-yellow to reddish grey	Thick-medium bedding	Fluvio-deltaic to transitional

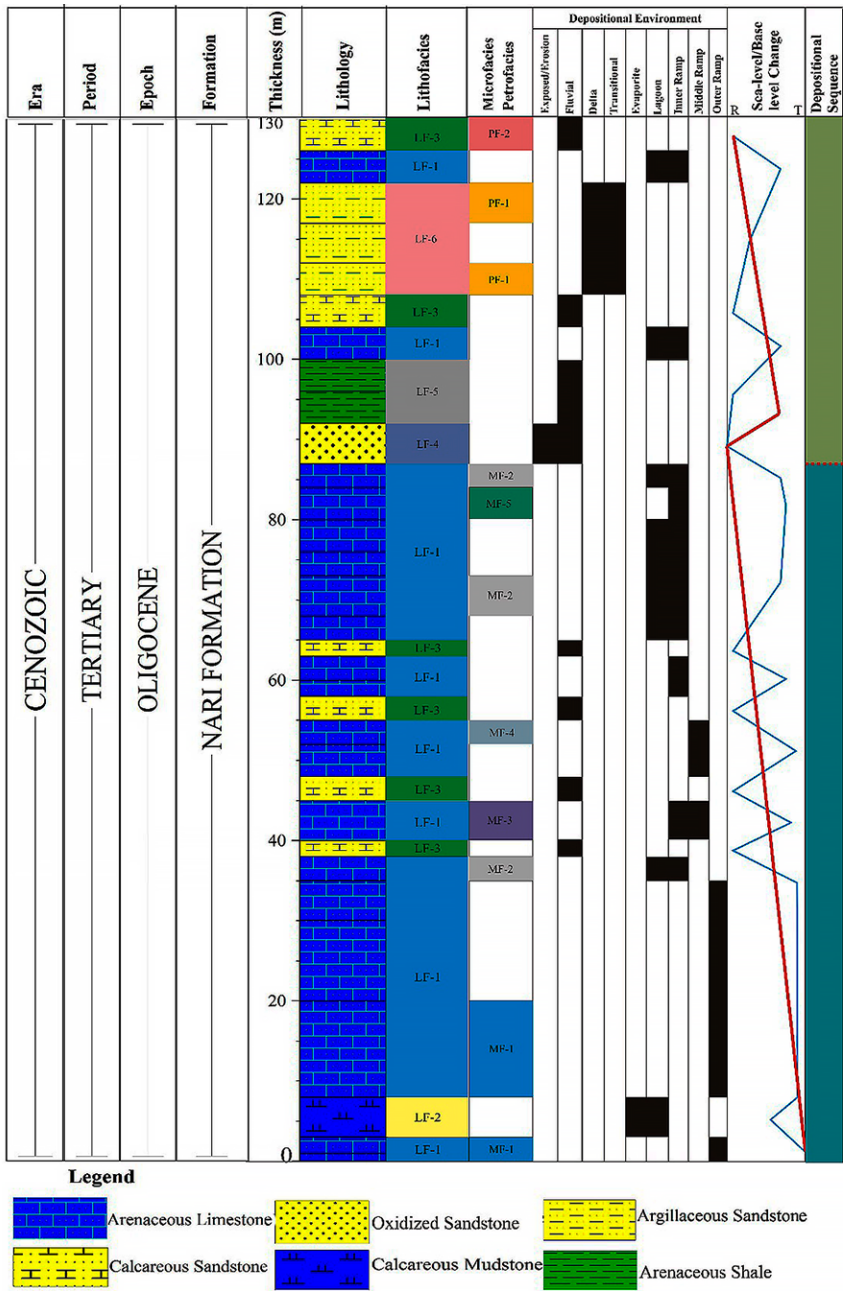

Figure 4. Graphic Log of the Nari Formation, showing identified facies, microfacies (MF), Petrofacies (PF-1), their depositional environments, sea-level (blue line), mean base level (red line) change pattern, (R=regression and T=transgression) and interpreted depositional sequences.

4.2 Calcareous-Gypsiferous Mudstone Facie (LF-2)

Description: This is the second lithologic unit of the Nari Formation in the study area, located immediately above the first bed of LF-1 (Figures 4, 5b). This facie may represent the contact between the underlying Late Eocene Kirthar Formation and the overlying Nari Formation. However, the first bed of LF-1 is included in the Nari Formation due its closer resemblance to the Nari Formation lithology rather than that of the Kirthar Formation (Figure 5a-b). The mudstone is soft and easily eroded, leaving behind the harder limestone ridges on its both sides. Therefore, this facie forms a depression between LF-1 strata and is covered with terrace deposits and vegetation and is only observed in drainage gullies (Figure 5b). Both the upper and lower bedding planes of this unit are sharp and erosional. The facie contains calcite nodules, gypsum laminations and veins, and in some places, iron concretions.

Interpretation: Such mudstones are typically deposited in shallow, low-energy water bodies, such as flood-plains, lakes or lagoons, where fine sediments settle from slow-moving or quite-water (Selley, 2000; Boggs, 2009; Lawal & Hassan 2023). The calcareous content indicates high calcium content in the water (Selley 2000; Anan 2014). The gypsum points towards arid to semi-arid conditions with high evaporation and limited freshwater influx (Melvin 1991; Könitzer et al. 2014). The occasional presence of iron concretions suggest oxidizing conditions (Nichols, 2009). These evidences suggest deposition in a shallow-water evaporative lagoon.

4.3 Calcareous Sandstone Facies (LF-3)

Description: These are the second most abundant facies, comprise six strata with a total thickness of 17 meters. The strata exhibit a range of colors,

such as dark brown, greenish grey, dark brown, reddish brown, yellowish grey and yellowish brown. The sandstone is fine to medium grained, in places coarse-grained, poor to moderately compact and thin to thick-bedded. These facies are relatively softer than the LF-1 and primary sedimentary structures are not observed in these facies. Both LF-1 and LF-3 alternate each other in the central part of the Nari Formation in study area (Figure 5d).

Interpretation: Variations in color may reflect climatic oscillations between wet and dry periods, changes in water chemistry, oxidation conditions or early diagenesis (Turner 1986; Tucker, 1988; Nichols, 2009; Zeller et al. 2015; Henares et al. 2020). The absence of primary structures indicates possible bioturbation, implying reworking of sediments by organisms during deposition. These observations points to a dynamic transitional to shallow marine depositional environment, potentially encompassing repetitive episodes of sediment reworking and deposition.

4.4 Laterite/Oxidized Sandstone Facie (LF-4)

Description: This facie is observed in the upper part of the Nari Formation in the study area, which comprises a 5 meter thick unit of laterite or oxidized sandstone. The facie is distinct in the field due to its distinct reddish-brown to blackish-red color and iron concretions and nodules. This facie is covered with pediment in the study area and its thickness is only measureable in the drainage gullies (Figure 5e).

Interpretation: This facie marks a phase of regression and sub-aerial exposure, allowing intense oxidation and tropical weathering (Walker 1974; Ikhane et al. 2022). Lateritization occurs due to chemical weathering of iron-bearing minerals in tropical to subtropical climates, especially with seasonal rainfalls (Schwarz 1996; Scholle et al. 2015; Nkoungou et al. 2023).

4.5 Arenaceous Shale Facies (LF-5)

Description: Two shale units with a combined thickness of 8 meters immediately overlie the oxidized sandstone unit (LF-4) (Figures 4, 5e-f).

- The lower shale unit exhibits dirty grey weathered and light grey when fresh, showing fissility, which is much similar to cross-stratification. It has erosional lower bedding plane (Figure 5f).
- The upper shale unit displays a dirty yellow weathered color and light yellow fresh color. This unit exhibit fissility and is nodular in places.

Interpretation: The fissility and erosional lower bedding plane suggest fluvial or deltaic deposition under inconsistent water flow, possibly influenced by periodic flooding events or increased sediment supply (Tucker, 2001; Boggs, 2009; Jadoon et al. 2017). The erosional lower bedding plane could be indicative of erosional processes during transgression phase (Nichols, 2009; Prothero & Schwab, 2014; Könitzer et al. 2014). The arenaceous nature and nodularity indicates that the upper shale unit might have been deposited during periodic desiccation and shrink-swell processes (Selley, 2000; Boggs, 2009; Abouelresh & Slatt 2011). The depositional environment for these shale units likely imitates transition from more vigorous with inconsistent fluvial water flow (lower shale unit) to somewhat more stable, periodically desiccating transitional environment (upper shale unit).

4.6 Argillaceous Sandstone Facies (LF-6)

Description: These are the third dominant facies, comprise three consecutive strata located near the top of the formation, with total thickness of 15 meters (Figures 4, 5e). The argillaceous sandstone is reddish-yellow to reddish grey, moderately to well compacted, in places friable, thick to medium-bedded and lacks primary sedimentary structures.

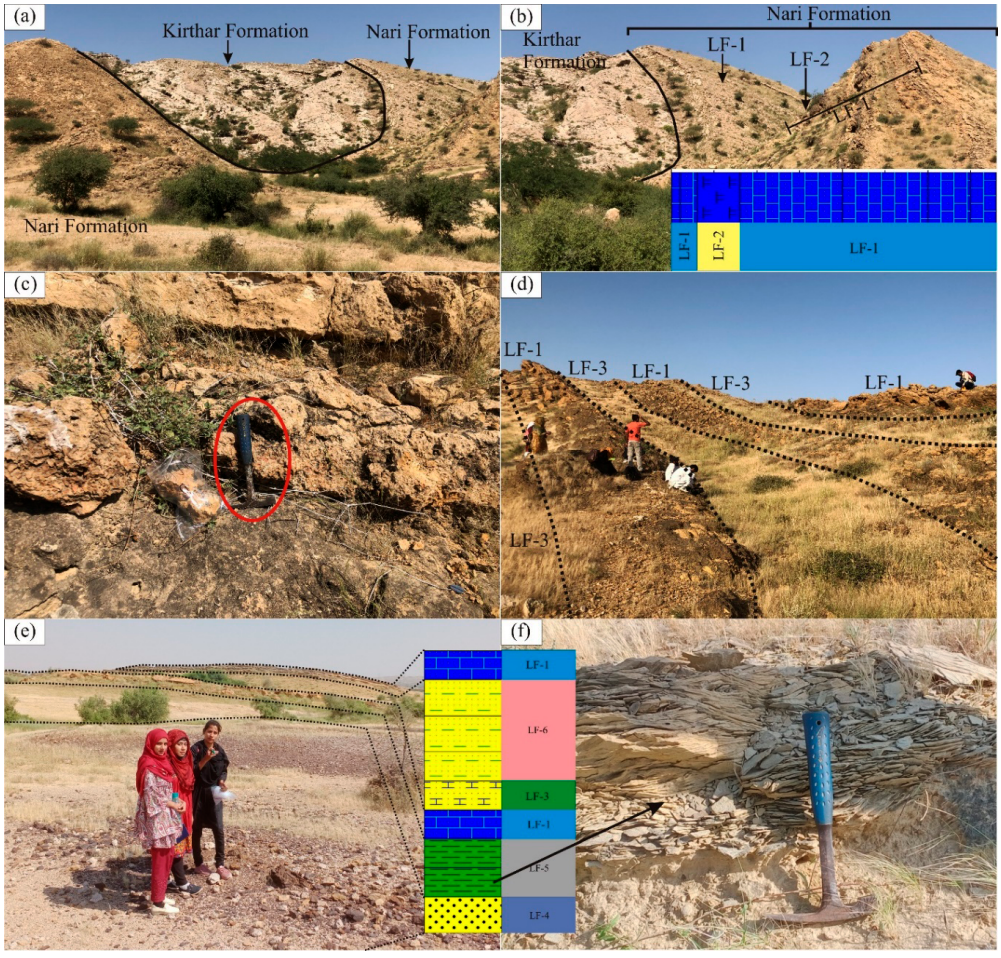

Figure 5. Field photographs showing [a] Contact of the Kirthar Formation and Nari Formation, [b] Basal facies of the Nari Formation, where calcareous-gypsiferous mudstone facies (LF-2) forms a depression between arenaceous limestone facies (LF-1), [c] Arenaceous limestone facies (LF-1), [d] Alternation of arenaceous limestone facies (LF-1) and calcareous sandstone facies (LF-3) in the central part of the Nari Formation, [e] Oxidized sandstone or laterite (LF-4) and overlying facies in the upper part of the Nari Formation, [f] fissility in the arenaceous shale (LF-5).

Interpretation: Argillaceous sandstone suggests the paleo-environment that combines elements of both sandstone and mudstone deposition, typically fluvio-deltaic, estuarine and tidal mud flats (Blatt et al., 1980; Sinclair 1993; Tucker, 2001). The mixing of marine and riverine processes suggest deposition under transitional conditions, specifically in quieter, more mud-dominated portions of deltaic setting (Selley, 2000; Duval, 2002; Boggs, 2006; Nichols, 2009; Yijun et al. 2010; Power et al. 2013; Ekwenye et al., 2014). The deposition of argillaceous sandstone is indicative of complex inter-relationship between fluvio-deltaic and transitional marine conditions (Blatt et al., 1980; Reading, 1996; Srivastava & Mankar 2015).

5. Petrography

5.1 Texture

Four textural attributes of limestone-dominated microfacies, i.e. allochems, lime mud or micrite, siliciclastic grains and sparry calcite are determined. Whereas, three textural attributes of sandstone-dominated petrofacies, i.e. framework grains, cement and matrix, are determined under the petrographic microscope (Table 2). The limestone-dominated microfacies are classified as "packed biomicrite" and "sparse biomicrite" according to Mount (1985) whereas sandstone-dominated petrofacies are classified as "arenites" according to Dott (1964), on the basis of textural attributes (Figure 7a-b). The term "allochem" was introduced by Folk (1962) to describe all carbonate aggregates that make up bulk of many limestones. In the identified microfacies, allochems consists of bioclasts, extraclasts and gluconite mineral grains (Figure 6). The bioclasts comprise whole organisms as well as fragments of foraminifera, mollusca, bryozoa, ostracoda, echinodermata and algae. Most of the bioclasts are affected by micritization (Figure 6a). The extraclasts are identified only in few samples of the Nari Formation, which show the signatures of transportation as well as alteration to micrite along their margins (Figure 6b). Lime mud or micrite is the second most dominant textural component of the limestone-dominated microfacies, which occurs as cement and matrix of these rocks (Figure 6c-d). Some units are dominantly composed of micrite (Figure 6d). The matrix of the microfacies is also made up of very fine skeletal fragments, quartz, silt and argillaceous materials. Sparry calcite constitute the cementing media along with micrite. Micrite is the most common cementing material, while sparry calcite is only observed in four samples as fibrous cement (Figure 6e). The occurrence of quartz, feldspar and other siliciclastic components in the studied sediments of the Nari Formation are believed to be terrigenous sediments (Figure 6f). The siliciclastics form wide size range from coarse sand to clay. Shape varies from angular to rounded, which indicates the varied distances of transport as well as intensity of reworking. The sandstone-dominated petrofacies are texturally immature, and are dominantly composed of sand, silt and clay-sized particles with minor carbonate allochems and micrite (Table 2).

5.2 Mineral Composition

The mineral composition of the Nari Formation from Hundi anticline is tabulated in Table 3. Calcite is the most dominant mineral in the studied samples. It ranges from 85 to 95% in limestone-dominated microfacies and 10 to 15% in sandstone-dominated petrofacies (Table 3). Majority of the calcite occurs as either skeletal debris or micrite, while occasionally it occurs as extraclasts and sparry calcite (Figures 6b-e). Calcite in the sandstone generally occurs as cementing material that fills inter-granular spaces (Figures 8a, c, g).

Table 2. The textural composition as calculated during petrography of the Nari Formation from Hundi Anticline, Karachi Embayment, Pakistan.

S. No.	Sample No.	Microfacies	Lithology	Textural Composition					Classification Mount (1985)	Standard Microfacies	Facies Zone
				Allochem (Bioclasts)	Micrite	Sand	Extraclast	Sparry Calcite			
1	HNR-1	MF-1	Arenaceous Limestone	75	20	5			Packed Biomicrite	SMF-10	Zone 7
2	HNR-4	MF-1	Arenaceous Limestone	70	22	8		Traces	Packed Biomicrite	SMF-10	Zone 7
3	HNR-7	MF-2	Arenaceous Limestone	15	82	3		Traces	Sparse Biomicrite	SMF-19	Zone 8
4	HNR-9	MF-3	Arenaceous Limestone	90	5	3	Traces	2	Packed Biomicrite	SMF-18	Zone 7
5	HNR-12	MF-4	Arenaceous Limestone	70	25	5	Traces	Traces	Packed Biomicrite	SMF-9	Zone 7
6	HNR-18	MF-2	Arenaceous Limestone	35	60	5	Traces		Sparse Biomicrite	SMF-19	Zone 8
7	HNR-21	MF-5	Arenaceous Limestone	70	22	8			Packed Biomicrite	SMF-19	Zone 8
8	HNR-22	MF-2	Arenaceous Limestone	25	70	5			Sparse Biomicrite	SMF-19	Zone 8
		Petrofacies		Frame-work Grains	Cement	Matrix	Cement type		Classification		
9	HNR-28	PF-1	Argillaceous Sandstone	68	21	11	Calcite, clay minerals		Arenite		
10	HNR-30	PF-2	Argillaceous Sandstone	70	20	10	Calcite, clay minerals		Arenite		
11	HNR-32	PF-3	Calcareous Sandstone	72	16	12	Calcite, clay minerals		Arenite		

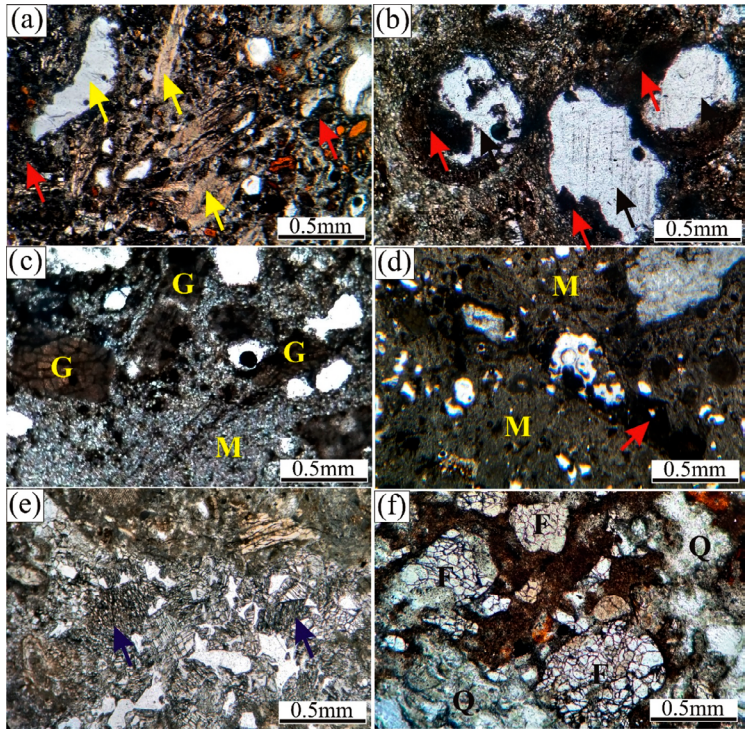

Figure 6. Photomicrographs of the Nari Formation showing different textural attributes as identified during the petrography [a] Yellow arrows showing bioclast allochems and red arrows show micritization of bioclasts, [b] Black arrows show calcite extraclasts and red arrows show their micritization, [c] Gluconite (G) in micrite (M)-rich sample, [d] Sample dominantly composed of micrite (M), while red arrow shows micritization of bioclast, [e] Blue arrows show sparry calcite, [f] Quartz (Q) and Feldspar (F) in argillaceous sandstone, where dark patches consists of clay minerals.

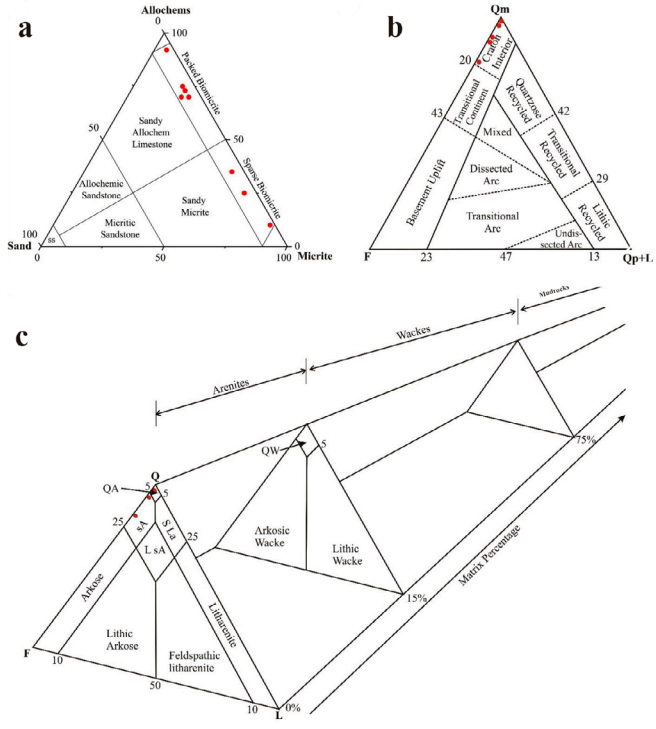

Figure 7..Ternary plots showing [a] Textural classification of the limestone-dominated facies of the Nari Formation, adopted after Mount (1985), [b] Textural and compositional classification of the sandstone-dominated facies of the Nari Formation, adopted after Mcbride (1963) and Dott (1964), [c] Tectonic setting of the clastic source area of the Nari Formation, adopted after Dickinson et al. (1983). (Abbreviations; F-Feldspar, L-Lithics, L sA-Lithic Sub-arkose, Q-Quartz, QA-Quartz Arenite, Qm-Monocrystaline Quartz, Qp-Polycrystaline Quartz, QW-Quartz Wacke, sA-Sub-arkose, S La-Sub-litharenite).

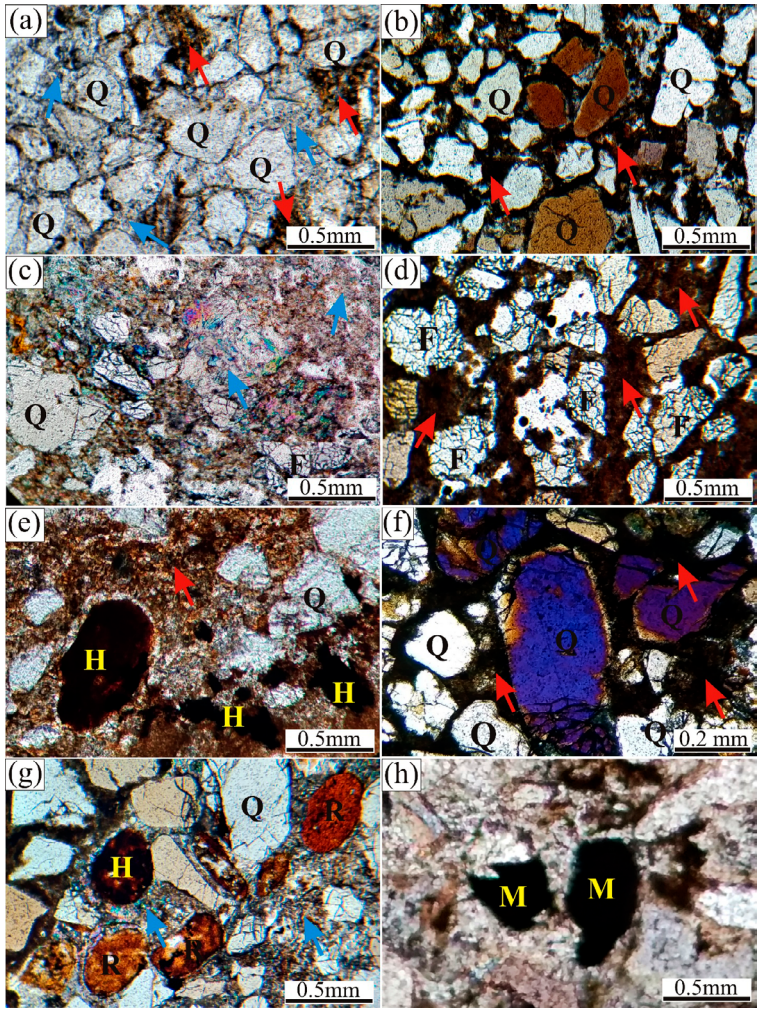

Figure 8. Photomicrographs of the Nari Formation showing different minerals as identified during the petrography [a] Calcite (blue arrows) and clay minerals (red arrows) as cementing material in quartz (Q) rich sandstone, [b] Quartz as framework minerals and clay minerals (red arrows) as cement, [c] Occurrence of framework calcite (blue arrows), quartz (Q) and feldspar (F) in arenaceous limestone, [d] Occurrence of feldspar (F) cemented with clay minerals (red arrows) in sandstone, [e] Clay minerals (red arrows) and hematite (H) in argillaceous sandstone, [f] Quartz (Q) cemented with clay minerals (red arrows) in argillaceous sandstone, [g] Traces of rutile (R) and hematite (H) in calcareous sandstone, where quartz (Q) is framework mineral and calcite is cement (blue arrows), [h] Traces of magnetite (M) in sandstone.

Table 3. The mineral composition as calculated during petrography of the Nari Formation from Hundi Anticline, Karachi Embayment, Pakistan.

S. No.	Sample No.	Micro/ Petro-facies	Lithology	Mineral Composition in Percentage								
				Calcite	Quartz	Feldspar	Clay Minerals	Hematite	Gluconite	Rutile	Pyrite	Magnetite
1	HNR-1	MF-1	Arenaceous Limestone	90	10	Traces		Traces	Traces			
2	HNR-4	MF-1	Arenaceous Limestone	90	8	1		1	Traces	Traces		
3	HNR-7	MF-2	Arenaceous Limestone	85	12	3						
4	HNR-9	MF-3	Arenaceous Limestone	92	8	Traces		Traces	Traces			
5	HNR-12	MF-4	Arenaceous Limestone	90	10	Traces		Traces	Traces	Traces		

S. No.	Sample No.	Micro/ Petro-facies	Lithology	Mineral Composition in Percentage								
				Calcite	Quartz	Feldspar	Clay Minerals	Hematite	Gluconite	Rutile	Pyrite	Magnetite
6	HNR-18	MF-2	Arenaceous Limestone	95	5			Traces				
7	HNR-21	MF-5	Arenaceous Limestone	85	13			2				
8	HNR-22	MF-2	Arenaceous Limestone	85	10	Traces		Traces	5		Traces	
9	HNR-28	PF-1	Argillaceous Sandstone	10	72	5	12	1		Traces		Traces
10	HNR-30	PF-2	Argillaceous Sandstone	10	72	8	10	Traces		Traces		Traces
11	HNR-32	PF-3	Calcareous Sandstone	15	85	Traces	Traces	Traces				Traces

The studied sediments of the Nari Formation dominantly contain non-undulose and mono-crystalline quartz (Figures 8a, b, f). The quartz ranges from 5 to 13% in the limestone-dominated microfacies (Figure 8c) while sandstone-dominated petrofacies contain 72 to 85% of quartz (Table 3). The second most dominant mineral in the sandstone is feldspar, which ranges from traces to 3% in limestone-dominated microfacies (Figure 8c), while traces to 8% in sandstone dominated petrofacies (Figure 8d) (Table 3). The feldspar grains are generally smoky, cloudy and in places show evidences of dissolution and alteration. The significant proportion of clay minerals are also observed in the sandstone-dominated petrofacies (Figures 8b, d) (Table 3). Gluconite is identified in five samples of the limestone-dominated microfacies in the range of traces to 5% (Table 3) (Figure 6c). Sediments of the Nari Formation contains minor to traces of hematite, rutile, pyrite and magnetite (Figures 8e-h) (Table 3). Hematite is observed in most of the studied samples from traces to 2% (Figure 8e).

6. Microfacies/Petrofacies Analysis

The studied samples are classified into five limestone-dominated microfacies and two sandstone-dominated petrofacies based on fossil contents, the relative abundance of allochems, micrite and framework grain composition. The identified microfacies and petrofacies are discussed below:

6.1 Discocyclina Packed Biomicrite Microfacies (MF-1)

Description: These are lowermost microfacies, which are identified in sample numbers HNR-1 and HNR-4 in basal part of the Nari Formation (Figure 4). These microfacies are part of the "arenaceous limestone facies (LF-1)" and are rich in *Discocyclina* and other larger benthic foraminifera (Figures 9a-e). The *Discocyclina* were earlier reported from the Nari Formation (Hunting Survey Corporation, 1960; Khan, 1968 Cheema *et al.,* 2009). These microfacies are dominantly composed of allochems, whereas micrite is observed to be in the range of 20-22% (Table 2). Both the allochems and micrite are composed of calcite, whereas, minor to trace occurrence of quartz, feldspar, hematite and glauconite are also observed (Table 3). Micritization and deformation of the bioclasts are also observed in these microfacies (Figures 9d-e).

Interpretation: The abundance of larger and flat benthic foraminifera, such as *Discocyclina* and allochems supports the low to moderate-energy, nutrient-rich depositional conditions. The Eocene-Oligocene wackstones rich in *Discocyclina* are deposited in the middle to outer ramp below the fair-weather wave base at 50–60 m water depth are reported by Zohdi et al. (2013) from Zagros Basin of Iran, Ali et al. (2018) from Suleiman Range of the Indus Basin, Pakistan, Banerjee et al. (2018) and Srivastava & Singh (2019) from the Kutch Basin of western India. Therefore, it is interpreted that these microfacies were deposited in the photic zone of middle to outer-ramp in the open-shelf platform (Figure 4). Micritization and deformation of bioclasts could be diagenetic in origin, rather than depositional. These microfacies correspond to SMF-10, deposited in facies zone 7, which is "open marine depositional zone" (Figure 12) (Wilson, 1975; Flugel, 2004; Boggs, 2009).

6.2 Sparse Biomicrite Microfacies (MF-2)

Description: These microfacies are observed in samples HNR-7, HNR-18 and HNR-22, and are part of the "arenaceous limestone facies (LF-1)" (Figure 4). Texturally immature these microfacies are dominantly composed of micrite and skeletal debris, with scarce fossil content (Table 2) (Figures 9f-I). Additionally, sparry calcite, calcite veins, fine quartz and feldspar are observed in sample HNR-7 (Table 3) (Figure 9g), calcite extraclasts in samples HNR-18 (Figure 6b), glauconite and traces of pyrite are observed in sample HNR-22 (Figure 9h).

Interpretation: The abundance of micrite indicate deposition in low-energy environment. The skeletal debris could belong to the remains of echinoderm, brachiopods and bivalves, which live in a variety of shallow marine environments (Scholle et al., 1983; Scholle & Ulmer-scholle, 2003). Scarcity of fossils in mudstone suggests an inner ramp lagoon depositional environment (Burchette & Wright, 1992). Fine-grained quartz and feldspar are strong evidence of deposition in low-energy conditions. The feldspar and pyrite indicate the anerobic (reducing) environment, while glauconite is indicative of slow-deposition (Amorosi, 1993). Therefore, it is interpreted that these microfacies were deposited in inner platform/lagoon with sporadic influxes of quartz, feldspar and calcite extraclasts from adjacent area (Figure 4). These microfacies are correlative with the SMF 19 (Flugel, 2004; Boggs, 2009), deposited in the facies zone 8, which is "platform interior restricted" (Figure 12).

6.3 Bivalve-Algae Packed Biomicrite Microfacies (MF-3)

Description: These microfacies are observed in sample HNR-9, and are part of the "arenaceous limestone facies (LF-1)". These are dominantly composed of allochems, which consists of formaninferal tests, skeletal fragments and calcareous algae. Minor proportion of the micrite, sand, sparry calcite and calcite veins are also identified (Table 2) (Figures 4, 6e, 10a). The allochems and micrite are composed of calcite, whereas minor proportion of quartz is observed (Table 3). These contain many varieties of microfossils such as foraminifera, bivalves, ostracods and calcareous algae. The foraminifera include *Nummulites, Miliolina*, *Alveolina*, *Fusulinina, Rotalia*, *Triloculina, Operculina* and *Gaudryina* etc (Figures 10a-g).

Interpretation: The abundance of allochems and scarcity of micrite suggests a high-energy hydrodynamic system under shallow marine environment produced either by tides or by combined tidal and wave processes during deposition of these microfacies (Srivastava & Singh, 2019). The presence

of broken *Nummulites* tests (Figure 10g) indicates deposition in turbulent water, which facilitated reworking of sediments. The fossils of bivalves indicates the shoal environment (Abd El-Moghny & Afifi, 2022). The presence of calcareous algae indicates middle ramp depositional setting (Singh et al., 2010; Zohdi et al., 2013), while foraminiferal tests suggests high-energy middle ramp depositional environment (Gischler et al., 2003; Beavington-Penney & Racey, 2004; Scheibner et al., 2007; Kumar et al., 2011; Zohdi et al., 2013; Banerjee et al., 2018). Therefore, it is interpreted that MF-3 were deposited in the middle ramp depositional setting (Figure 4). These microfacies are equivalent to SMF-18 of (Wilson, 1975; Flugel, 2004), deposited in the facies zone 7 which is "open marine depositional zone" (Figure 12).

6.4 Assilina-Operculina Packed Biomicrite Microfacies (MF-4)

Description: These microfacies are observed in sample HNR-12, and are part of the "arenaceous limestone facies (LF-1)". They contain fossils of *Assilina*, *Operculina, Nummulites* and rare Bryozoans (Figures 4, 10h-m). These microfacies are dominantly composed of allochems and micrite is observed to be 25% (Table 2). The micritization of the skeletal fragments is commonly observed in these microfacies. The allochems and micrite are composed of calcite, whereas, minor occurrence of quartz is also observed (Table 3).

Interpretation: Significant proportion of allochems indicate deposition under medium to high energy depositional environment. The good preservation of the *Assilina*, *Operculina* and *Nummulites* suggest deposition below the fair-weather wave base. The association of *Assilina*, *Operculina* and *Nummulites* fossils is indicative of deposition under medium to high energy middle to outer ramp environment (Beavington-Penney & Racey, 2004; Scheibner et al., 2007; Kumar et al., 2011; Zohdi et al., 2013; Banerjee et al., 2018; Abd El-Moghny & Afifi, 2022). These microfacies are correlated with the SMF 9 (Wilson, 1975) (Flugel, 2004), deposited in the facies zone 7 (Figure 12).

6.5 Arenaceous Packed Biomicrite Microfacies (MF-5)

Description: These microfacies are identified in sample HNR-21, and are last fossil-bearing microfacies of the Nari Formation in studied section (Figure 4). These are characterized by presence of significant amount of sand, micrite and fossils of *Camerina* and *Miliolina* (Figures 11a-b). The sand and fossils consists of the allochem of these microfacies, which are dominantly composed of calcite with minor proportion of quartz and hematite (Tables 2, 3).

Interpretation: The *Camerina* and *Miliolina* indicate shallow marine inner ramp depositional environment (Nikbakht et al., 2019; Alam et al., 2023). Furthermore, presence of significant micrite indicates low-energy depositional environment, which also had received clastic influx from the nearby environment (Khan et al., 2018; Rizwan et al. 2020). Therefore, the MF-5 is interpreted to be deposited in semi-restricted inner ramp depositional environment (Figure 4). These microfacies can be compared with the SMF 19 (Wilson 1975; Flugel 2004), deposited in the facies zone 8 (Figure 12).

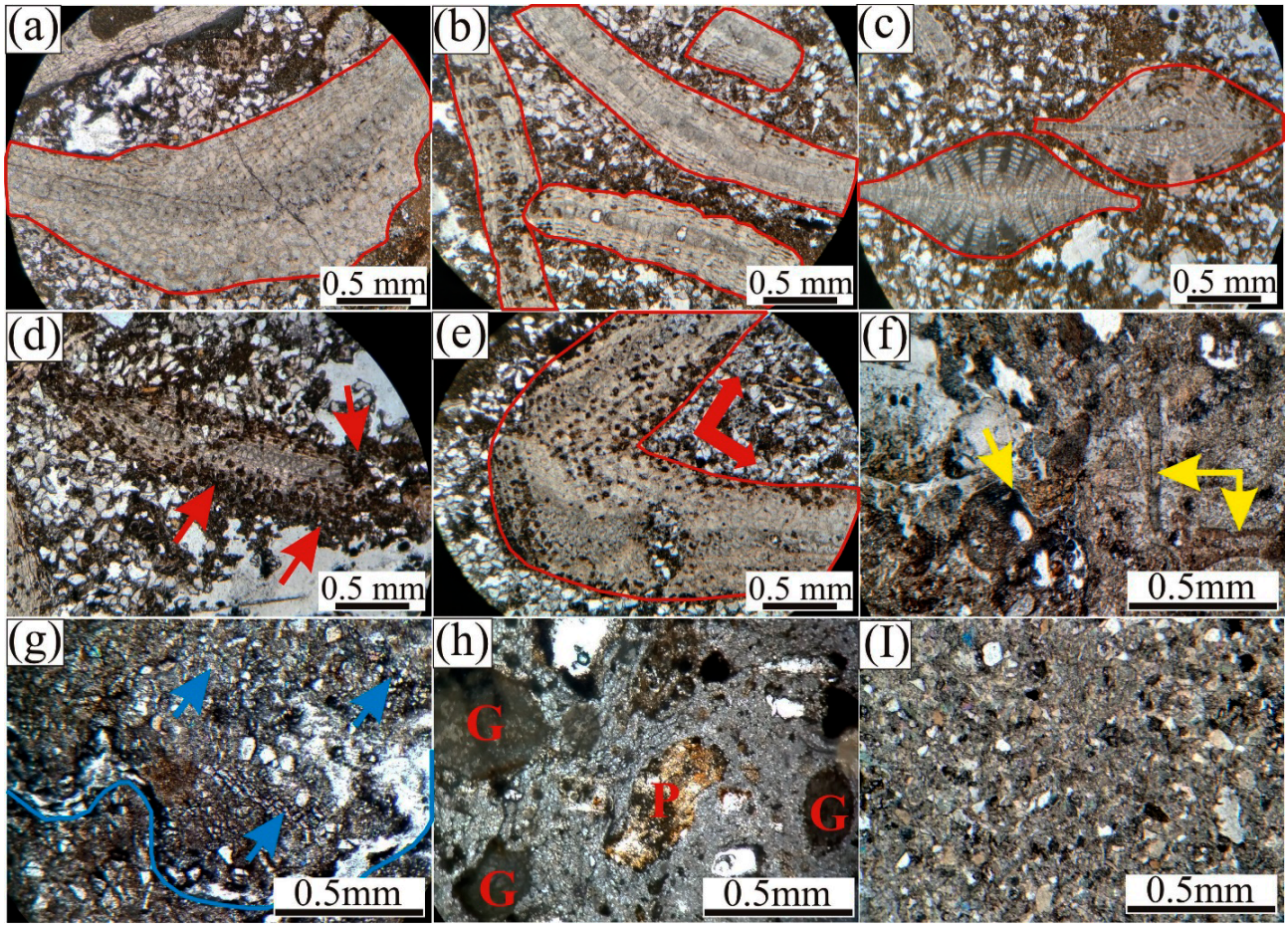

Figure 9. Photomicrographs of the Nari Formation showing [a-c] Occurrence of *Discocyclina* in MF-1, [d] Micritization of *Discocyclina* bioclast, [e] Folded *Discocyclina* bioclast, [f] Skeletal debris in MF-2, [g] Sparry calcite (blue arrow) and calcite vein (blue line), [h] Glauconite (G) and pyrite (P) embedded in micrite framework, [I] Micrite in sparse biomicrite microfacies.

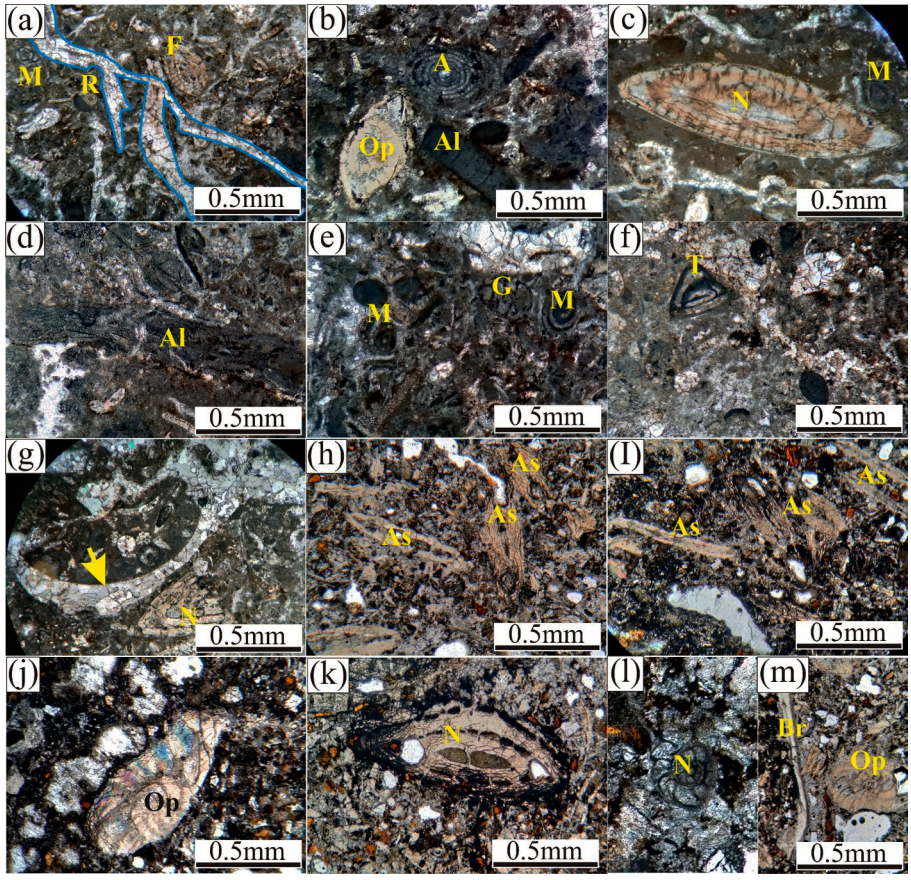

Figure 10. Photomicrographs of the Nari Formation showing [a] Microfossils of *Miliolina* (M), *Rotalia* (R), *Fusulinina* (F) and calcite veins (blue line), [b] *Alveolina* (A), *Operculina* (O) and Algae (Al), [c] *Nummulites* (N) and *Miliolina* (M), [d] Alage (Al), [e] *Gaudryina* (G) and *Miliolina* (M), [f] *Triloculina* (T), [g] Cross-sectional view of bivalve (yellow arrow and fragment of *Nummulites* (N), [h-i] *Assilina* (As), [j] *Operculina* (Op), [k-l] *Nummulites* (N), [m] *Operculina* (Op) and Bryozoa (Br).

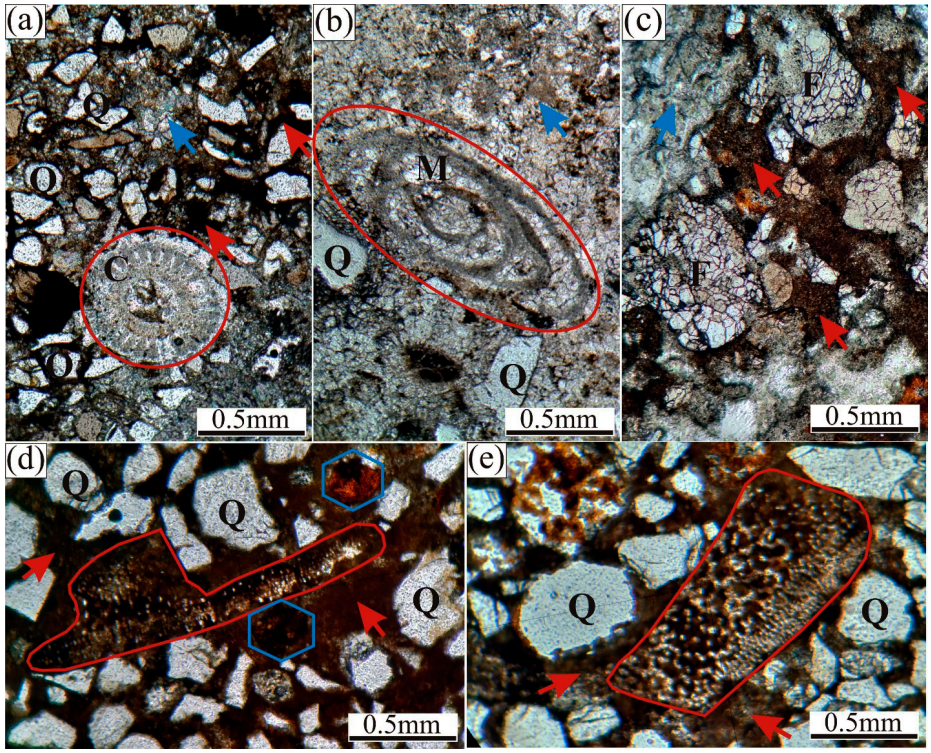

Figure 11. Photomicrographs of the Nari Formation showing [a] *Camerina* (C), quartz (Q) micrite (red arrows) and calcite (blue arrow), [b] *Miliolina* (M), quartz (Q) and (blue arrow) cement, [c] Feldspar (F), calcite (blue arrow) and clay minerals (red arrow) cement (yellow arrow), [d-e] Quartz (Q), algae (red polygons), clay minerals (red arrows) and hematite grains (blue hexagons).

6.6 Sub-arkose Sandstone Petrofacies (PF-1)

Description: The sub-arkose sandstone petrofacies are identified in samples HNR-28 and HNR-30, and belong to "argillaceous sandstone facies (LF-6)" (Figure 4). Texturally as well as mineralogicaly, these petrofacies are immature, composed of quartz, calcite, feldspar, clay minerals and traces of hematite, magnetite, rutile and algae (Figure 8 and 11c-e; Table 3). The quartz and feldspar are framework grains, which are fine-grained sub-angular to sub-rounded and poorly sorted. The framework mineral grains are cemented with calcite and clay minerals. The cementing material occurs as either continues framework, veins or patches (Figures 11d-e).

Interpretation: The texture of these petrofacies indicate moderate transportation and deposition in low-energy condition (Boggs, 2006; Reading, 2009). The presence of algae suggest transitional, whereas traces of iron-bearing minerals are indicative of oxidizing conditions (Khan et al., 2018; Alam et al., 2023). Therefore, it is interpreted that these petrofacies were deposited in fluvio-deltaic to transitional conditions (Boggs, 2009) (Nichols 2009; Sallam et al. 2018; Rizwan et al. 2020) (Figure 12).

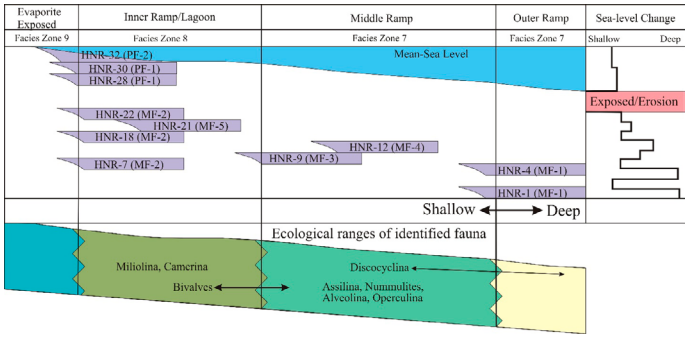

Figure 12. Interpreted depositional environments of identified microfacies and petrofacies of the Nari Formation in studied section with respect to ecological ranges of identified fauna.

6.7 Quartz Arenite Petrofacies (PF-2)

Description: These petrofacies are recognized in the sample HNR-32, and belong to "calcareous sandstone facies (LF-3)". These are composed of quartz with minor feldspar, hematite and magnetite (Figure 4; Table 3). The calcite and clay minerals occur as cementing material. The quartz grains are floating in the calcite cement, while clay minerals occur as isolated patches (Figures 8a-b). The quartz is fine-grained, sub-angular to sub-rounded and poorly sorted. Texturally, these petrofacies are immature, whereas mineralogicaly, these are relatively more mature than PF-1.

Interpretation: Fine-grained and poorly sorted quartz with absence of fossils suggests the low-energy depositional conditions. The presence of calcite cement reflects the connection to marine environment. The patches of clay minerals along with calcite suggest the depositional environment was periodically flooded with storms (Blatt et al. 1980; Blatt 1985; Boggs 2006; Nikbakht et al., 2019). The absence of fossils in these petrofacies further support the interpretation of unfavorable conditions for the preservation of organic material and development of biotic communities. The turbid water and fluctuating salinity due to periodic water inflows may have hindered the growth of living habitat (Nikbakht et al., 2019; Alam et al., 2023). Therefore, it is interpreted that these petrofacies were deposited in low-energy transitional to lagoon setting (Figure 12).

7. Discussion

7.1 Clastic Source

The lithic fragments are rarely observed in petrofacies of the Nari Formation. On the basis of relative proportion of quartz (Q), feldspar (F) and lithics (L), the argillaceous sandstone petrofacies are classified as "sub-arkose", whereas calcareous sandstone petrofacies are classified as "quartz arenite" (Figure 7b) (Mcbride, 1963). Quartz and feldspar are essential components of acidic plutonic rocks (Pettijohn 1975; Madukwe et al. 2014; Wang et al. 2017). Their abundance suggests that the sandstone clasts of the Nari Formation were derived from acidic plutonic igneous sources. This interpretation is in agreement with the provenance of older clastic rocks in the study area, where clasts were supplied by granites and granitic-gneisses of the Indian Craton, exposed to the east and southeast (Hakro et al., 2018; Hakro et al., 2021; Hakro et al., 2022; Hakro et al., 2023; Thebo et al., 2023).

The tectonic setting of the clastic source area is interpreted using the framework mineral composition of sandstone, plotted on a ternary diagram adopted after Dickinson et al. (1983). The relationship between sandstone framework composition and tectonic setting indicates that the clasts present in the Nari Formation were derived from a craton interior setting (Figure 7c). The association of feldspar and clay minerals in the studied samples indicates that clay minerals formed through feldspar alteration. The low concentration of feldspar and rare rock fragments in the samples indicate a prolonged chemical weathering of the source area, likely under warm and humid climatic conditions (Pettijohn et al., 1987; Amireh, 1991; Hakro et al. 2023; Bilal et al. 2023b).

7.2 Depositional Environment

7.2.1 Carbonate-dominated Facies: Outer to Inner Ramp Settings

The lower part of the Nari Formation is dominated by arenaceous limestone (LF-1), which comprises the carbonate microfacies (MF-1 to MF-5) identified during present study. The LF-1 indicates a shallow-marine platform with limited clastic input and abundant biological activity. The presence of larger benthic foraminifera such as *Discocyclina, Assilina* and *Operculina* (MF-1 and MF-4) suggests deposition under low to moderate-energy conditions, specifically within outer to middle ramp settings below the fair-weather wave base (Srivastava & Singh (2019; Nikbakht et al., 2019; Alam et al., 2023; Shah et al., 2024). The MF-3 represents higher energy conditions, as manifested by abundant skeletal fragments and calcareous algae, which is in good agreement with middle ramp to shoal or back-shoal settings (Burchette & Wright, 1992; Rizwan et al. 2020). The MF-2 and MF-5 microfacies indicate low-energy environments in the inner ramp or semi-restricted lagoon settings. Rare fossil content, high micrite proportion, occurrence of feldspar, glauconite and pyrite support deposition in a quit, semi-restricted inner ramp, sometimes under anaerobic conditions (Khan et al., 2018; Rizwan et al. 2020).

The LF-1 marks transgression at its base, because these facies are deposited in relatively deeper waters than underlying facies. Therefore seven transgression phases are identified at the base of these facies within the Nari Formation (Figure 4). These are the only facies, which mark the transgression at their base while all other five facies (LF-2 to LF-6) are deposited during regressive phases. The presence of calcareous-gypsiferous mudstone (LF-2) between the (LF-1), in the base of the Nari Formation suggest evaporative lagoon conditions during the early phase of its deposition. The facies pattern indicates that despite an initial phase of uplift and regression (LF-2), the early deposition of Nari Formation occurred in relatively stable basin (LF-1) (Figure 13).

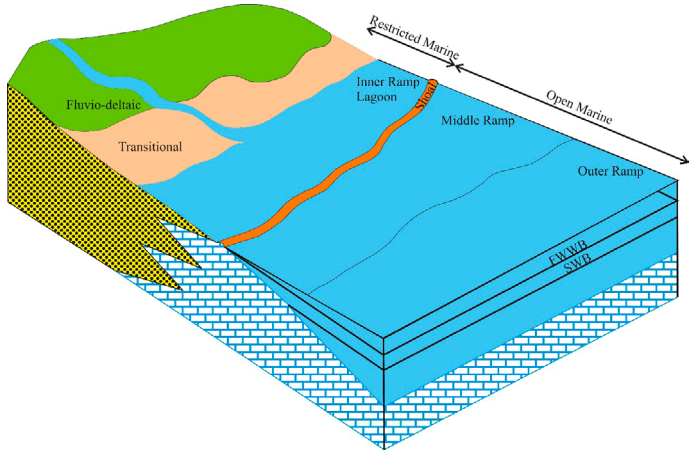

Figure 13. Schematic depositional model of the Oligocene Nari Formation from Hundi anticline, Karachi Embayment, Indus Basin, Pakistan.

7.2.2 Clastic-dominated Facies: Inner Ramp to Fluvio-deltaic Settings

Up-section, calcareous sandstone (LF-3) and oxidized sandstone/laterite (LF-4) reflect more dynamic environments with intermittent exposure and weathering under tropical climatic influences. The LF-3 facies are represented by quartz arenite petrofacies (PF-2). The PF-2, characterized by high quartz content, calcite cement and absence of fossils, indicates deposition in a low-energy, periodically storm-influenced lagoon (Srivastava & Mankar 2015; Ahmad et al., 2021). The most common alternation of LF-1 and LF-3 suggest the periodic repetition of depositional conditions in which both these facies were deposited in a nearly same depositional environment, e.g. inner ramp to semi-restricted lagoon (Figures 4, 5d, 13). The deposition of LF-1 (MF-5 and MF-2) after LF-3 culminated in the exposure and development of laterite/oxidized sandstone (LF-4). It marked end of the first depositional sequence of the Nari Formation, which was dominantly composed of shallow-marine platform sediments.

The second depositional sequence of the Nari Formation is dominantly composed of transitional to fluvio-deltaic sediments. The arenaceous shale facies (LF-5) mark a transition from continental (LF-4) to transitional settings, influenced by episodic flooding and desiccation. These facies are overlain by arenaceous limestone (LF-1), deposited in the semi-restricted inner ramp lagoon settings. Therefore, their stratigraphic position suggests that the arenaceous shale facies were deposited in a fluvio-deltaic to transitional stage during the sea level rise (Figure 4). The repetition of LF-1 and LF-3 in the upper part of the Nari Formation suggest periodic return of the inner ramp/lagoon settings. The LF-3 is overlain by the argillaceous sandstone facies (LF-6), which aligns with the sub-arkose petrofacies (PF-1). The fine-grained quartz, feldspar, clay minerals and algae traces suggest a low-energy fluvio-deltaic to transitional environment (Rizwan et al. 2020; Ahmad et al., 2021; Babkir et al., 2023). Traces of algal remains and iron-bearing minerals point to shallow oxidizing conditions. Furthermore, association of LF-6 with LF-1 and LF-3, suggest desiccation and estuarine to fluvio-deltaic sedimentation under regressive conditions.

The transition of facies from one environment to adjacent environment suggests that the Nari Formation was deposited on the homoclinal carbonate ramp, where depositional environments graded from deeper outer ramp settings to inner ramp lagoons and fluvio-deltaic conditions without major slope breaks (Burchette & Wright, 1992) (Figure 13). Overall, the vertical facies progression document a regressive depositional system and transition from shallow-marine to fluvio-deltaic conditions, potentially driven by plate collision during the Oligocene. Bender (1995) suggested that marine conditions in the Indus Basin started to retreat during the Late Eocene and Early Oligocene. The depositional pattern of the Nari Formation indicates that basin was experiencing transitional phase from a passive-margin to a foreland basin. The regular clastic supply to the carbonate depositional system also confirms the tectonic uplift and deformation. These observations suggest that the early stage of deformation of the northwestern margin of the Indian Plate during Oligocene had profound control on the depositional environment in the study area.

8. Conclusions

The Oligocene Nari Formation in the study area comprises six carbonate-clastic facies, including arenaceous limestone, calcareous sandstone, argillaceous sandstone, laterite/oxidized sandstone, arenaceous shale and calcareous mudstone. Petrographic analysis further identified five limestone-dominated microfacies (packed and sparse biomicrites) and two sandstone-dominated petrofacies (sub-arkose and quartz arenite). The framework composition of the sandstone indicates a clastic source linked to the granitic terrains of the Indian Craton. The facies succession displays a general progradational pattern, deposited in a range of environments on the homoclinal ramp, including outer ramp, middle ramp, inner ramp, lagoon, evaporate, transitional and fluvio-deltaic. This vertical facies pattern indicates a regressive depositional system and transition from shallow-marine to fluvio-deltaic conditions, driven by the Himalayan orogeny associated with collision of the Indian and Eurasian Plates during the Oligocene.

Acknowledgements

Authors are thankful to the Centre for Pure and Applied Geology, University of Sindh, Jamshoro, for providing the transport and logistical support to carry out the fieldwork for present study. Authors are also thankful to the students Mrs. Muskan Lodhi, Mrs. Zahida Lashari, Mrs. Komal Sheikh and Mr. Abdul Subhan Ghouri for their assistance during the measurement of stratigraphic section and sampling in the field as well as laboratory.

We sincerely thank the editorial board of the "Earth Sciences Research Journal" for their efficient handling of our manuscript. We also extend our gratitude to the anonymous reviewers for their thoughtful, critical and constructive feedback, which greatly improved the quality of this work.

Author contributions

Surriya Bibi Ahmedani: Conceptualization, Writing original draft, Asghar A. A. D. Hakro: Conceptualization, Resources, Supervision, Abdul Shakoor Mastoi: Methodology, Supervision, Investigation, Aijaz Ali Halepoto: Data curation, Formal analysis, Ali Ghulam Sahito: Visualization, Validation, Software, Shamim Akhtar: Review and Editing, Rafique Ahmed Lashari: Methodology, Supervision and Review.

Declaration of Competing Interest

The data used in this study is taken from the outcrops, which are open data sources. Therefore, it is declared that we have no any conflict of interest to disclose. Meanwhile where published data sets are used, the reference of the authors are given. Work described here has not been published previously in any journal and not under consideration for publication elsewhere.

Funding:

This research did not receive any specific grant from funding agencies in the public, commercial, or not-for-profit sectors.

Data Availability Statement

The data that support the findings of this study are available from the corresponding author upon reasonable request.

References

Abd El-Moghny, M. W., & Afifi, A. A. (2022). Microfacies analysis and depositional environments of the Middle Eocene (Bartonian) Qurn Formation along Qattamiya—Ain Sokhna district, Egypt. *Carbonates and Evaporites*, *37*(1), 1–16. https://doi.org/10.1007/s13146-022-00762-9

Abouelresh, M., & Slatt, R. (2011). Shale depositional processes: Example from the Paleozoic Barnett Shale, Fort Worth Basin, Texas, USA. *Open Geosciences*, *3*(4), 398–409.

Aguilera-Franco, N., & Romano, U. H. (2004). Cenomanian–Turonian facies succession in the Guerrero–Morelos Basin, Southern Mexico. *Sedimentary Geology*, *170*(3–4), 135–162.

Ahmad, F., Quasim, M. A., & Ahmad, A. H. M. (2021). Microfacies and diagenetic overprints in the limestones of Middle Jurassic Fort Member (Jaisalmer Formation), Western Rajasthan, India: Implications for the depositional environment, cyclicity, and reservoir quality. *Geological Journal*, *56*(1), 130–151.

Ahmed, R., & Ahmed, J. (1991). Petroleum Geology and Prospects of Sukkur Rift Zone, Pakistan with Special Reference to Jaisalmer, Cambay and Bombay High Basins of India. *Pakistan Journal of Hydrocarbon Research*, *3*(2), 33–41.

Ahmed, S., Solangi, S. H., Jadoon, M. S. K., & Nazeer, A. (2018). Tectonic evolution of structures in Southern Sindh Monocline, Indus Basin, Pakistan formed in multi-extensional tectonic episodes of Indian Plate. *Geodesy and Geodynamics*, *9*(2), 358–366.

Ahmed, Z., Khan, A. S., & Ahmed, B. (2020). Sandstone Composition and Provenance of the Nari Formation, Central Kirthar Fold belt, Pakistan. *Pakistan Journal of Geology*, *4*(2), 90–96. https://doi.org/10.2478/pjg-2020-0010

Ahmedani, S. B., Agheem, M. H., Hakro, A. A. A. D., Halepoto, A. A., Lashari, R. A., & Thebo, G. M. (2024a). Integrated Petrographical, Mineralogical and Geochemical Investigation to Evaluate Diagenesis of Sandstone: A Case Study of the Oligocene Nari Formation from Southern Kirthar Range, Pakistan. *Journal of Himalayan Earth Sciences*, *57*(1), 1–22.

Ahmedani, S. B., Lashari, R. A., Hakro, A. A. A. D., Mastoi, A. S., Agheem, M. H., & Halepoto, A. A. (2024b). Repeating Lithological Diversity of Clastics, Carbonates and Evaporites as Herald of Depositional Instability: An Outcrop-based Interpretation of Nari Formation from Northern Ranikot Anticline, Sindh, Pakistan. *7th International Earth Sciences Pakistan Conference, Baragali Summer Campus, University of Peshawar, Abbotabad, Pakistan*, 20–21.

Alam, S. ul, Mohibullah, M., Kasi, A. K., Abdullah, A., Hussain, T. M., & Thebo, G. M. (2023). Microfacies analysis, Depositional Environment and Biostratigraphy of the Early Eocene Dungan Formation, Kohlu area Balochistan, Pakistan. *Journal of Himalayan Earth Sciences*, 56(2), 89–104.

Al-Bassam, K., Magna, T., Vodrážka, R., & Čech, S. (2019). Mineralogy and geochemistry of marine glauconitic siliciclasts and phosphates in selected Cenomanian–Turonian units, Bohemian Cretaceous Basin, Czech Republic: Implications for provenance and depositional environment. *Geochemistry*, *79*(2), 347–368.

Ali, N., Özcan, E., Yücel, A. O., Hanif, M., Hashmi, I., Ullah, F., Rizwan, M., & Pignatti, J. (2018). Bartonian orthophragminids with new endemic species from the Pirkoh and Drazinda formations in the Sulaiman Range, Indus Basin, Pakistan. *Geodinamica Acta*, *30*(1), 31–62. https://doi.org/10.1080/09853111.2017.1419676

Allemann, F. (1979). Time of Emplacement of the Zhob Valley Ophiolites and Bela Ophiolites, Baluchistan (Preliminary Report). In A. Farah and K. A. De Jong (Eds.), *Geodynamics of Pakistan* (pp. 215–242). Geological Survey of Pakistan.

Amireh, B. S. (1991). Mineral Composition of the Cambrian-Cretaceous Nubian Series of Jordan: Provenance, Tectonic Setting and Climatological Implications. *Sedimentary Geology*, *71*, 99–119.

Amorosi, A. (1993). Use of Gluconites for Stratigraphic Correlation: A Review and Case Studies. *Gioranle Di Geologia*, *55*, 117–137.

Anan, T. I. (2014). Facies analysis and sequence stratigraphy of the Cenomanian–Turonian mixed siliciclastic–carbonate sediments in west Sinai, Egypt. *Sedimentary Geology*, *307*, 34–46.

Babkir H. B. M. D., Nton, M. E., & Eisawi, A. A. (2023). Depositional environment and hydrocarbon exploration potential based on sedimentary facies and architectural analysis of the Upper Cretaceous Shendi Formation in Musawwarat-Naga area, Shendi-Atbara Basin, Sudan. *Earth Sciences Research Journal*, 27(2), 109-128.

Banerjee, S., Khanolkar, S., & Saraswati, P. K. (2018). Facies and depositional settings of the Middle Eocene-Oligocene carbonates in Kutch. *Geodinamica Acta*, *30*(1), 119–136. https://doi.org/10.1080/09853111.2018.1442609

Bannert, D., Cheema, A., Ahmed, A., & Schaffer, U. (1992). The Structural Development of the Western Fold Belt, Pakistan. *Geologisches Jahrbuch Reihe*, *B80*, 3–60.

Barron, E. J., & Harrison, C. G. A. (1980). An analysis of past plate motions; the South Atlantic and Indian oceans. In P. A. Davies and S. K. Runcorn (Eds.), *Mechanisms of continental drift and plate tectonics* (pp. 89–109). Academic Press: London.

Bathurst, R. G. C. (1971). *Carbonate Sediments and their Diagenesis* (Developmen). Elsevier, Amsterdam.

Beavington-Penney, S. J., & Racey, A. (2004). Ecology of extant nummulitids and other larger benthic foraminifera: Applications in palaeoenvironmental analysis. *Earth-Science Reviews*, *67*(3–4), 219–265. https://doi.org/10.1016/j.earscirev.2004.02.005

Bender, F. K. (1995). Paleogeographic and Geodynamic Evolution. In F. K. Bender and H. A. Raza (Eds.), *Geology of Pakistan* (pp. 162–181). Gebruder Borntraeger.

Bender, F. K., & Raza, H. A. (Eds.). (1995). *Geology of Pakistan*. Gebruder Borntraeger.

Besse, J., & Courtillot, V. (1988). Paleogeographic maps of the continents bordering the Indian Ocean since the Early Jurassic. *Journal of Geophysical Research*, *93*(B10), 791–808.

Bilal, A., Yang, R., Janjuhah, H. T., Mughal, M. S., Li, Y., Kontakiotis, G., & Lenhardt, N. (2023). Microfacies analysis of the Palaeocene Lockhart limestone on the eastern margin of the Upper Indus Basin (Pakistan): Implications for the depositional environment and reservoir characteristics. *Depositional Record*, *9*(1), 152–173. https://doi.org/10.1002/dep2.222

Bilal, A., Yang, R., Lenhardt, N., Han, Z., & Luan, X. (2023). The Paleocene Hangu formation: A key to unlocking the mysteries of Paleo-Tethys tectonism. *Marine and Petroleum Geology*, *157*(September), 106508. https://doi.org/10.1016/j.marpetgeo.2023.106508

Blanford, W. T. (1876). On the Geology of Sind. *Geological Survey of India*, *Rec. 9*, 8–22.

Blanford, W. T. (1879). The Geology of western Sind. *Geological Survey of India*, *Memoir 17*, 1–196.

Blatt, H. (1985). Provenance studies and mudrocks. *Journal of Sedimentary Petrology*, *55*, 69–75.

Blatt, H., Middleton, G. V, & Murray, R. C. (1980). *Origin of sedimentary rocks*. Prentice Hall.

Boggs, S. J. (2006). *Principles of Sedimentology and Stratigraphy* (4th ed.). Pearson Prentice Hall.

Boggs, S. J. (2009). *Petrology of Sedimentary Rocks*. cambridge University Press.

Brandano, M., & Ronca, S. (2014). Depositional processes of the mixed carbonate–siliciclastic rhodolith beds of the Miocene Saint-Florent Basin, northern Corsica. *Facies*, *60*(1), 73–90.

Burchette, T. P., & Wright, V. P. (1992). Carbonate Ramp Depositional Systems. *Sedimentary Geology*, *79*, 3–57.

Burret, C. F. (1974). Plate Tectonics and the fusion of Asia. *Earth and Planetary Science Letters*, *21*, 181 – 189.

Cheema, M. R., Ahmed, H., & Raza, S. M. (2009). Cenozoic. In S. M. I. Shah (Ed.), *Stratigraphy of Pakistan* (Mem. 22, pp. 237–308). Geological Survey of Pakistan.

Cheema, M. R., Raza, S. M., & Ahmed, H. (1977). Cenozoic. In S. M. I. Shah (Ed.), *Stratigraphy of Pakistan* (Mem.12, pp. 56–97). Geological Survey of Pakistan.

Coe, A. L., Argles, T. W., Rothery, D. A., & Spicer, R. A. (2010). *Geological Field Techniques* (A. L. Coe (Ed.)). Wiley-Blackwell.

Compton, R. R. (1962). *Manual of Field Geology*. John Wiley and Sons.

Coward, M. P., Butler, R. W. H., Chambers, A. F., Graham, R. H., Izatt, C. N., Khan, M. A., Knipe, R. J., Prior, D. J., Treloar, P. J., & Williams, M. P. (1988). Folding and imbrication of the Indian crust during Himalayan collision. *Philosophical Transactions of the Royal Society of London*, *326*, 89–116. https://doi.org/10.1098/rsta.1988.0081

Curiale, J. A., Covington, G. H., Shamsuddin, A. H. M., Morelos, J. A., & Shamsuddin, A. K. M. (2002). Origin of petroleum in Bangladesh. *AAPG Bulletin*, *86*(4), 625–652. https://doi.org/10.1306/61eedb66-173e-11d7-8645000102c1865d

Della Porta, G., Mancini, A., & Berra, F. (2023). Facies character and evolution of a mixed carbonate–siliciclastic shelf: Upper Triassic–Lower Jurassic succession in the eastern Northern Calcareous Alps (Stumpfmauer, Austria). *Facies*, *69*(3), 11.

Devey, C. W., & Lightfoot, P. C. (1986). Volcanological and tectonic control of stratigraphy and structure in the western Deccan traps. *Bulletin of Volcanology*, *48*(4), 195–207. https://doi.org/10.1007/BF01087674

Dickinson, W. R., Beard, G. R., & Brakenridge. (1983). Provenance of North American Phanerozoic Sandstone in relation to Tectonic Setting. *Geological Society of America Bulletin*, *94*, 222–235.

Dott, R. H. (1964). Wacke, Graywacke and Matrix-What Approach to Immature Sandstone Classification? *Journal of Sedimentary Petrology*, 34(3), 625–632. https://doi.org/10.1306/74d71109-2b21-11d7-8648000102c1865d

Doyle, L. J., & Roberts, H. H. (1988). *Carbonate–Clastic Transitions*. Elsevier, Amsterdam.

Duncan, P. M., & Sladen, W. P. (1884). Tertiary and Upper Cretaceous fossils of western Sind; Fasc. 4, the fossil Echinoidea from the Nari Series, the Oligocene formation of western Sind. *Geological Survey of India Memmoir Paleontologica Indica, Series 14*, *1*(3), 242–272.

Duval, B. B. (2002). *Sedimentary Geology: Sedimentary Basins, Depositional Environments, Petroleum Formation*. Technip, Paris.

Ekwenye, O. C., Nichols, G. J., Collinson, M., Nwajide, C. S., & Obi, G. C. (2014). A paleogeographic model for the sandstone members of the Imo Shale , south-eastern Nigeria. *Journal of African Earth Sciences*, *96*, 190–211. https://doi.org/10.1016/j.jafrearsci.2014.01.007

Flugel, E. (2004). *Microfacies of Carbonate Rocks: Analysis, Interpretation and Application*. Springer Berlin Heidelberg.

Folk, R. L. (1962). Spectral subdivision of limestone types. In W. E. Ham (Ed.), *Classification of Carbonate Rocks* (AAPG Memoir, pp. 62–84). American Association of Petroleum Geologists.

Fowler, J. N., Graham, R., Smewing, J. D., Warburton, J., & Sassi, W. (2004). Two-dimensional Kinematic Modeling of the Southern Kirthar Fold Belt, Pakistan. In R. Swennen, F. Roure, and J. W. Granath (Eds.), *Deformation, fluid flow, and reservoir appraisal in foreland fold and thrust belts* (pp. 117–131). AAPG Hedberg Series, No.1,. https://doi.org/10.1306/1025688H13112

Ghani, H., Hinsch, R., Sobel, E. R., & Glodny, J. (2023). Oligocene to Pliocene structural evolution of the frontal Kirthar fold and thrust belt of Pakistan. *Journal of Structural Geology*, *176*, 1–10. https://doi.org/10.1016/j.jsg.2023.104961

Gil-Gil, J., Bretones, A., Boix, C., & García-Hidalgo, J. F. (2024). Evolution of coniacian facies and environments in the Iberian basin: a longshore current controlling siliciclastic sand distribution on a carbonate platform. *Facies*, *70*(2), 7.

Gischler, E., Hauser, I., Heinrich, K., & Scheitel, U. (2003). Characterization of depositional environments in isolated carbonate platforms based on benthic foraminifera, Belize, Central America. *Palaios*, *18*(3), 236–255.

Greensmith, J. T. (1981). *Petrology of Sedimentary Rocks* (6th ed.). George Allen and Unwin Limited.

Hakro, A. A. A. D., Samtio, M. S., Mastoi, A. S., & Rajper, R. H. (2021). The Major Elemental Composition of Middle Paleocene Sediments of Southern Indus Basin Pakistan: Implication on Provenance. Earth Science Malaysia, 5(1), 01–09. https://doi.org/10.26480/esmy.01.2021.01.09

Hakro, A. A. A. D., Xiao, W., Mastoi, A. S., Yan, Z., Samtio, M. S., & Rajper, R. H. (2021). Grain size analysis of the Oligocene Nari Formation sandstone in the Laki Range, southern Indus Basin, Pakistan: Implications for depositional setting. *Geological Journal*, *56*(11), 5440–5451. https://doi.org/10.1002/gj.4251

Hakro, A. A. A. D., Ali, S., Mastoi, A. S., Rajpar, R. H., Awan, R. S., Samtio, M. S., Xiao, H., & Lu, X. (2023). Mineralogy and element geochemistry of the Sohnari rocks of Early Eocene Laki Formation in the Southern Indus Basin , Pakistan: Implications for paleoclimate , paleoweathering and paleoredox conditions. *Energy Geoscience*, *4*(1), 143–157. https://doi.org/10.1016/j.engeos.2022.09.002

Hakro, A. A.A.D., Xiao, W., Yan, Z., & Mastoi, A. S. (2018). Provenance and tectonic setting of Early Eocene Sohnari Member of Laki Formation from southern Indus Basin of Pakistan. *Geological Journal*, *53*(5), 1854–1870. https://doi.org/10.1002/gj.3011

Hakro, A. A. A. D., Samtio, M. S., Rajper, R. H., & Mastoi, A. S. (2022). Major Elements of Nari Formation Sandstone from Jungshahi Area of Southern Indus Basin, Pakistan. *Pakistan Journal of Scientific and Industrial Research Series A: Physical Sciences*, *65A*(3), 248–259.

Halepoto, A. A., Agheem, M. H., Hakro, A. A., Ahmed, S., & Ahmedani, S. B. (2025). Lateral strike-slip deformation and possible transition of extensional faults to strike-slip faults in the foreland fold belt: a regional to outcrop tectonic synthesis of the Southern Kirthar Fold Belt, northwestern Indian Plate, Pakistan. *Journal of Asian Earth Sciences*, 291(106678), 1-27. https://doi.org/10.1016/j.jseaes.2025.106678

Halepoto, A. A., Ahmed, S., Agheem, M. H., Hakro, A. A. A. D., Lashari, R. A., & Ahmedani, S. B. (2023). Integrated Study of Structural Styles and their Suitability for Hydrocarbon Entrapment, Southern Kirthar Fold Belt, Pakistan. *Journal of Physics: Conference Series*, *2594*, 1–12. https://doi.org/10.1088/1742-6596/2594/1/012021

Halepoto, A. A., Ahmed, S., Agheem, M. H., Hakro, A. A. A. D., Lashari, R. A., & Ahmedani, S. B. (2022). Assessment of Suitability for Hydrcarbon Entrapment in the Ranikot Anticline, Southern Kirthar Fold Belt (SKFB), Pakistan. *PAPG-SPE Annual Technical Conference 2022, Islamabad, Pakistan*, 35–48.

Haqbin, M., Inanch, S., Qarizada, K., & Qarizada, D. (2024). Unveiling the Geological Significance and Industrial Application of Limestone: A Comprehensive Review. *The Journal of The Institution of Engineers Malaysia*, *85*(1).

Hedley, R., Warburton, J., & Smewing, J. (2001). Sequence Stratigraphy and Tectonics in the Kirthar Foldbelt, Pakistan. *PAPG/SPE Annual Technical Conference, 7-8 November 2001, Islamabad, Pakistan*, *November 2001*.

Henares, S., Donselaar, M. E., & Caracciolo, L. (2020). Depositional controls on sediment properties in dryland rivers: Influence on near-surface diagenesis. *Earth-Science Reviews*, *208*, 103297.

Hinsch, R., Asmar, C., Hagedorn, P., Nasim, M., Rasheed, M. A., Stevens, N., Bretis, B., & Kiely, J. M. (2018). Structural Modelling in the Kirthar Fold Belt of Pakistan: From Seismic to Regional Scale. *AAPG/SEG International Conference and Exhibition*.

Hunting Survey Corporation. (1960). *Reconnaissance Geology of Part of West Pakistan*. A Colombo Plan Co-operative Project.

Hussein, H. S., Bábek, O., Mansurbeg, H., & Shahrokhi, S. (2024). Outcrop-to-subsurface correlation and sequence stratigraphy of a mixed carbonate-siliciclastic ramp using element geochemistry and well logging; Upper Cretaceous Kometan Formation, Zagros Foreland, NE Iraq. *Sedimentary Geology*, *459*, 106547. https://doi.org/10.1016/j.sedgeo.2023.106547

Ikhane, P. R., Atewolara-Odule, O. C., Oyebolu, O. O., & Fakolade, O. R. (2022). Chemostratigraphic Architecture of Sandstone Facies Exposed along Auchi-Ighara Road, Mid-Western Nigeria. *GeoScience Engineering*, *68*(1), 33–45.

Ingersoll, R. V., Bullard, T. F., Ford, R. L., Grimm, J. P., Pickle, J. D., & Sares, S. W. (1984). The effect of grain size on detrital modes: A test of the Gazzi-Dickinson point-counting method. *Journal of Sedimentary Petrology*, 54(1), 0103–0116. https://doi.org/10.1306/212f8783-2b24-11d7-8648000102c1865d

Jadoon, I. A. K., Ding, L., Jadoon, S. K., Bhatti, Z. I., Shah, S. T. H., & Qasim, M. (2021). Lithospheric Deformation and Active Tectonics of the NW Himalayas, Hindukush and Tibet. *Lithosphere*, *2021*, 1–17.

Jadoon, I. A. K., Ding, L., Nazir, J., Idrees, M., & Jadoon, S. ur R. K. (2020). Structural interpretation of frontal folds and hydrocarbon exploration, western sulaiman fold belt, Pakistan. *Marine and Petroleum Geology*, *117*, 104380. https://doi.org/10.1016/j.marpetgeo.2020.104380

Jadoon, I. A. K., Lawrence, R. D., & Lillie, R. J. (1992). Balanced and Retrodeformed Geological cross-section from the frontal Sulaiman Lobe , Pakistan : Duplex Development in thick strata along the western margin of the Indian Plate. In K. R. McClay (Ed.), *Thrust Tectonics* (pp. 343–356). Chapman and Hall.

Jadoon, Q. K., Roberts, E. M., Henderson, B., Blenkinsop, T. G., Wüst, R. A. J., & Mtelela, C. (2017). Lithological and facies analysis of the Roseneath and Murteree shales, Cooper Basin, Australia. *Journal of Natural Gas Science and Engineering*, *37*, 138–168.

Jamrich, M., Rybár, S., Ruman, A., Kováčová, M., & Hudáčková, N. (2024). Biostratigraphy and paleoecology of the upper Badenian carbonate and siliciclastic nearshore facies in the Vienna Basin (Slovakia). *Facies*, *70*(1), 5.

Kadri, I. B. (1995). *Petroleum Geology of Pakistan*. Pakistan Petroleum Limited.

Kazmi, A. H., & Abbasi, I. A. (2008). Stratigraphy and Historical Geology of Pakistan. *National Centre of Excellence in Geology, University of Peshawar*, 524.

Kazmi, A. H., & Jan, M. Q. (1997). *Geology and Tectonics of Pakistan*. Graphic Publishers.

Kazmi, A. H., & Rana, R. A. (1982). *Tectonic Map of Pakistan*. Geological Survey of Pakistan, Quetta.

Khan, A. S., Kelling, G., Umar, M., & Kassi, A. M. (2002). Depositional environments and reservoir assessment of late cretaceous sandstones in the South central Kirthar foldbelt, Pakistan. *Journal of Petroleum Geology*, *25*(4), 373–406. https://doi.org/10.1111/j.1747-5457.2002.tb00092.x

Khan, M. H. (1968). The dating and correlation of the Nari and Gaj formation. *Geological Bulletin of Punjab Univiversity*, *7*, 57–65.

Khan, M., Khan, M. A., Shami, B. A., & Awais, M. (2018). Microfacies analysis and diagenetic fabric of the Lockhart Limestone exposed near Taxila, Margalla Hill Range, Punjab, Pakistan. *Arabian Journal of Geosciences*, 11(2). https://doi.org/10.1007/s12517-017-3367-4

Khokhar, Q. D., Hakro, A. A. A. D., Solangi, S. H., Siddiqui, I., & Abbasi, S. A. (2016). Textural Evaluation of Nari Formation , Laki Range , Southern Indus Basin , Pakistan. *Sindh University Research Journal (Science Series)*, *48*(3), 633–638.

Könitzer, S. F., Davies, S. J., Stephenson, M. H., & Leng, M. J. (2014). Depositional controls on mudstone lithofacies in a basinal setting: implications for the delivery of sedimentary organic matter. *Journal of Sedimentary Research*, *84*(3), 198–214.

Kumar, S. K., Chandrasekar, N., Seralathan, P., & Godson, P. S. (2011). Depositional environment and faunal assemblages of the reef-associated beachrock at Rameswaram and Keelakkarai Group of Islands, Gulf of Mannar, India. *Frontiers of Earth Science*, *5*(1), 61–69. https://doi.org/10.1007/s11707-011-0165-2

Lawal, M., & Hassan, M. H. A. (2023). Sedimentary and stratigraphic characteristics of the Maastrichtian Dukamaje formation of southern Iullemmeden Basin: Implications for the paleogeography of the Upper Cretaceous trans-Saharan seaway. *Journal of African Earth Sciences*, *200*, 104878.

Madukwe, H. Y., Akinyemi, S. A., Adebayo, O. F., Ojo, A. O., Aturamu, A. O., Afolagboye, L. O., & Abstract: (2014). Geochemical And Petrographic Studies Of Lokoja Sandstone: Implications On Source Area Weathering, Provenance, And Tectonic Setting. *International Journal of Scientific and Technology Research*, *3*(12), 21–32.

Mahmud, S. A., & Sheikh, S. A. (2009). Reservoir Potential of Lower Nari Sandstones (Early Oligocene) In Southern Indus Basin and Indus Offshore. *SPE/PAPG Annual Technical Conference*, *50582*(2012).

Mcbride, E. F. (1963). A Classification of Common Sandstones. *Journal of Sedimentary Petrology*, *34*, 661–673.

Mcloughlin, S. (2001). The breakup history of Gondwana and its impact on pre-Cenozoic floristic provincialism. *Australian Journal of Botany*, *49*, 271–300.

Meissner, C. R. J., & Rehman, H. (1973). Distribution, Thickness, and Lithology of Paleocene Rocks in Pakistan. *USGS. Professional Paper 716-E*, 6.

Melvin, J. L. (Ed.). (1991). *Evaporites, Petroleum and Mineral Resources* (Developmen). Elsevier.

Mount, J. (1985). Mixed Siliciclastic and Carbonate Sediments: A Proposed first-order Textural and Compositional Classification. *Sedimentology*, *32*, 435–442.

Nichols, G. (2009). *Sedimentology and Stratigraphy* (2nd ed.). Wiley-Blackwell.

Nikbakht, S. T., Rezaee, P., Moussavi-Harami, R., Khanehbad, M., & Ghaemi, F. (2019). Facies analysis, sedimentary environment and sequence stratigraphy of the Khan Formation in the Kalmard Sub-Block, Central Iran: implications for Lower Permian palaeogeography. *Neues Jahrbuch Für Geologie Und Paläontologie-Abhandlungen*, 292(2), 129–154. https://doi.org/10.1127/njgpa/2019/0812

Nkoungou, H. L. E., Tsala, S. A. Z., Oyoa, V., & Eba′ a Owoutou, P. (2023). Laterization Process Recognition along the Northern Border of the Congo Craton by Geoelectrical and Geotechnical Data. *International Journal of Geophysics*, *2023*(1), 8534774.

Odin, G. S., & Matter, A. (1981). Degluconiarum Origin. *Sedimentology*, *28*, 611–641.

Pettijohn, F. J. (1975). *Sedimentary Rocks* (3rd ed.). Harper and Row.

Pettijohn, F. J., Potter, P. E., & Siever, R. (1987). *Sand and Sandstone*. Springer-Verlag, New York.

Powell, C. M. (1979). A Speculative Tectonic History of Pakistan and Surroundings: Some constraints from Indian Ocean. In A. Farah and K. A. De Jong (Eds.), *Geodynamics of Pakistan* (pp. 5–24). Geological Survey of Pakistan.

Powell, C. M., Roots, S. R., & Veevers, J. J. (1988). Pre-breakup continental extension in East Gondwanaland and the early opening of the eastern Indian Ocean. *Tectonophysics*, *155*, 261–283.

Prothero, D. R., & Schwab, F. (2014). *Sedimentary Geology: An Introduction to Sedimentary Rocks and Stratigraphy* (3rd ed.). W. H. Freeman and Company.

Qasim, M., Tabassum, K., Ding, L., Tanoli, J. I., Awais, M., & Baral, U. (2022). Provenance of the Late Cretaceous Pab Formation, Sulaiman fold-thrust belt, Pakistan: Insight from the detrital zircon U–Pb geochronology and sandstone petrography. *Geological Journal*, 1–12. https://doi.org/DOI: 10.1002/gj.4546

Raza, H. A., Ali, S. M., & Ahmed, R. (1990). Petroleum Geology of Kirthar sub-Basin and Part of Kutch Basin. *Pakistan Journal of Hydrocarbon Research*, *2*(1), 29–73.

Reading, H.G. (Ed.). (1996). *Sedimentary Environments: Processes, Facies and Stratigraphy* (3rd ed.). Blackwell Science, Oxford.

Reading, H. G. (2009). *Sedimentary environments: processes, facies and stratigraphy*. John Wiley and Sons.

Rizwan, M., Hanif, M., Ali, N., & Rehman, M. U. (2020). Microfacies analysis and depositional environments of the Upper Cretaceous Fort Munro Formation in the Rakhi Nala Section, Sulaiman. *Carbonates and Evaporites*, *35*(104), 1–20. https://doi.org/10.1007/s13146-020-00639-9

Robles-Salcedo, R., & Vicedo, V. (2023). Palaeoenvironments of an Upper Cretaceous mixed carbonate-siliciclastic shelf of the external Prebetic domain (Valencia, SE Spain). *Facies*, *69*(3), 13.

Saker-Clark, M. (2019). *Early Jurassic Palaeoenvironmental Change–A North African Perspective*. The Open University.

Sallam, E. S., Issawi, B., Osman, R., & Ruban, D. A. (2018). Deposition in a changing paleogulf: evidence from the Pliocene–Quaternary sedimentary succession of the Nile Delta, Egypt. *Arabian Journal of Geosciences*, *11*, 50–58.

Samtio, M. S., Hakro, A. A. A. D., Lashari, R. A., Mastoi, A. S., Rajper, R. H., & Agheem, M. H. (2021). Depositional Environment of Nari Formation from Lal Bagh Section of Sehwan Area, Sindh Pakistan. *Sindh University Research Journal (Science Series)*, *53*(01), 67–76.

Sanders, D. (2003). Syndepositional dissolution of calcium carbonate in neritic carbonate environments: geological recognition, processes, potential significance. *Journal of African Earth Sciences*, *36*(3), 99–134.

Sarwar, G., & De Jong, K. A. (1979). Arcs, Oroclines, Syntaxes: the Curvatures of Mountain Belts in Pakistan. In A. Farah and K. A. De Jong (Eds.), *Geodynamics of Pakistan* (pp. 341–349). Geological Survey of Pakistan.

Sarwar, U., Ghazi, S., Ali, S. H., Mehmood, M., Khan, M. J., Zaheer, A., & Arif, S. J. (2024). Sedimentological and sequence stratigraphic analysis of Late Eocene Kirthar Formation, Central Indus Basin, Pakistan, Eastern Tethys. *Earth Sciences Research Journal*, *28*(1), 29–38. https://doi.org/10.15446/esrj.v28n1.108562

Scheibner, C., Rasser, M. W., & Mutti, M. (2007). The Campo section (Pyrenees, Spain) revisited: Implications for changing benthic carbonate assemblages across the Paleocene–Eocene boundary. *Palaeogeography, Palaeoclimatology, Palaeoecology*, *248*(1–2), 145–168.

Scholle, D. S. U., Scholle, P. A., Schieber, J., & Raine, R. J. (2015). Diagenesis: Iron Sulfide, Oxide and Hydroxide Cements. In D. S. Ulmer-Scholle, P. A. Scholle, J. Schieber, and R. J. Raine (Eds.), *A Color Guide to the Petrography of Sandstones, Siltstones, Shales and Associated Rocks* (Vol. 109). American Association of Petroleum Geologists. https://doi.org/10.1306/13521920M1093637

Scholle, P. A., Bebout, D. G., & Moore, C. H. (Eds.). (1983). *Carbonate Depositional Environments* (AAPG Memoi). American Association of Petroleum Geologists.

Scholle, P. A., & Ulmer-scholle, D. S. (2003). *A Color Guide to the Petrography of Carbonate Rocks: Grains, textures, porosity, diagenesis* (AAPG Memoi). The American Association of Petroleum Geologists.

Schwarz, T. (1996). GJJ Aleva (Compiler) Laterites. Concepts, Geology, Morphology and Chemistry. ISRIC, Wageningen, 1994. 169 pp. Price NLG 25. ISBN: 90.6672. 053.0. *Clay Minerals*, *31*(3), 440–441.

Selley, R. C. (2000). *Applied Sedimentology* (2nd ed.). Academic Press: London.

Shah, S. B. A., Ismail, K., & Bakar, W. Z. W. (2024). Integrated Analysis of the Eocene Sakesar Formation: Depositional Environment, Microfacies, Geochemistry, and Reservoir Characteristics in the Potwar Basin, Pakistan. *Earth Sciences Research Journal*, 28(1), 17-27.

Shah, S. M. I. (Ed.). (2009). *Stratigraphy of Pakistan* (Mem. 22). Geological Survey of Pakistan.

Shar, A. M., Mahesar, A. A., Abbasi, G. R., Narejo, A. A., & Hakro, A. A. A. D. (2021). Influence of diagenetic features on petrophysical properties of fine-grained rocks of Oligocene strata in the Lower Indus Basin, Pakistan. *Open Geosciences*, *13*, 517–531. https://doi.org/10.1515/geo-2020-0250

Shar, A. M., Mahesar, A. A., Narejo, A. A., & Fatima, N. (2021). Petrography and Geochemical Characteristics of Nari Sandstone in Lower Indus Basin, Sindh, Pakistan. *Mehran University Research Journal of Engineering and Technology*, *40*(1), 82–92. https://doi.org/10.22581/muet1982.2101.08

Shehata, A. A., Kassem, A. A., Brooks, H. L., Zuchuat, V., & Radwan, A. E. (2021). Facies analysis and sequence-stratigraphic control on reservoir architecture: Example from mixed carbonate/siliciclastic sediments of Raha Formation, Gulf of Suez, Egypt. *Marine and Petroleum Geology*, *131*, 105160.

Siddiqui, N. K. (2016). *Petroleum Geology, Basin Architecture and Stratigraphy of Pakistan*. Published by the Author.

Singh, S. K., Kishore, S., Misra, P. K., Jauhri, A. K., & Gupta, A. (2010). Middle Eocene calcareous algae from southwestern Kachchh, Gujarat. *Journal of the Geological Society of India*, *75*, 749–759.

Smewing, J. D., Warburton, J., Cernuschi, A., & Ul-Haq, N. (2002). Structural Inheritance in the Southern Kirthar Fold Belt. *PAPG/SPE Annual Technical Conference, 22-23 November 2002, Islamabad, Pakistan*.

Smewing, J. D., Warburton, J., Daley, T., Copestake, P., & Ul-Haq, N. (2002). Sequence Stratigraphy of the southern Kirthar Fold Belt and Middle Indus Basin , Pakistan. In P. D. Clift, D. Kroon, C. Gaedicke, and J. Craig (Eds.), *The Tectonic and Climatic Evolution of the Arabian Sea Region* (Special Pu, pp. 273–299). Geological Society of London.

Srivastava, A. K., & Mankar, R. S. (2015). Lithofacies architecture and depositional environment of Late Cretaceous Lameta Formation, central India. *Arabian Journal of Geosciences*, *8*(1), 207–226. https://doi.org/10.1007/s12517-013-1192-y

Srivastava, V. K., & Singh, B. P. (2019). Depositional environments and sources for the middle Eocene Fulra Limestone Formation, Kachchh Basin, western India: Evidences from facies analysis, mineralogy, and geochemistry. *Geological Journal*, *54*(1), 62–82. https://doi.org/10.1002/gj.3154

Thebo, G. M., Solangi, S. H., Agheem, M. H., Solangi, M. A., Markhand, A. H., & Memon, K. A. (2023). Petrography and Geochemistry of late Cretaceous Pab Sandstone, Laki range, Southern Indus Basin, Pakistan: implications for Provenance and Paleoclimate. *Journal of Himalayan Earth Sciences*, 56(1), 65–78.

Tong, Z., Hu, Z., Li, S., Huang, Y., Zuo, Y., Zhu, Y., Pang, Y., Dong, Q., & Xu, C. (2023). Silicate and carbonate mixed shelf formation and its controlling factors, a case study from the Cambrian Canglangpu formation in Sichuan basin, China. *Open Geosciences*, *15*(1), 20220480.

Tucker, M. E. (1988). *Techniques in Sedimentology*. Blackwell Scientific Publishing, Oxford.

Tucker, M. E. (2001). *Sedimentary Petrology: An Introduction to the Origin of Sedimentary Rocks* (3rd ed.). Blackwell Science Ltd.

Turner, B. R. (1986). Tectonic and climatic controls on continental depositional facies in the Karoo Basin of northern Natal, South Africa. *Sedimentary Geology*, *46*(3–4), 231–257.

Unrug, R. (1997). Rodinia to Gondwana: The Geodynamic Map of Gondwana Supercontinent Assembly. *GSA Today, A Publication of the Geological Society of America*, *7*(1), 1–6.

Walker, T. R. (1974). Formation of Red Beds in Moist Tropical Climates: A Hypothesis. *Bulletin of the Geological Society of America*, *85*(4), 633–638. https://doi.org/10.1130/0016-7606(1974)85<633:FORBIM>2.0.CO;2

Wang, Z., Wang, J., Fu, X., Feng, X., Wang, D., Song, C., Chen, W., & Zeng, S. (2017). Petrography and geochemistry of upper Triassic sandstones from the Tumengela Formation in the Woruo Mountain area , North Qiangtang Basin , Tibet : Implications for provenance , source area weathering , and tectonic setting. *Island Arc*, 26(4), 1–15. https://doi.org/10.1111/iar.12191

Williams, M. D. (1959). Stratigraphy of the Lower Indus Basin, West Pakistan. *Proceedings of the 5th World Petroleum Congress*, *Section I*(19), 377–391.

Wilson, J. L. (1975). *Carbonate Facies in Geologic History*. Springer Berlin Heidelberg.

Yijun, L. I., Yong, Z., Renchao, Y., Aiping, F. A. N., & Fuping, L. I. (2010). Detailed sedimentary facies of a sandstone reservoir in the eastern zone of the Sulige gas field, Ordos Basin. *Mining Science and Technology (China)*, *20*(6), 891–903.

Zecchin, M., Caffau, M., & Catuneanu, O. (2021). Recognizing maximum flooding surfaces in shallow-water deposits: An integrated sedimentological and micropaleontological approach (Crotone Basin, southern Italy). *Marine and Petroleum Geology*, *133*, 105225.

Zecchin, M., Catuneanu, O., & Caffau, M. (2023). High-resolution sequence stratigraphy of clastic shelves IX: Methods for recognizing maximum flooding conditions in shallow-marine settings. *Marine and Petroleum Geology*, *156*, 106468.

Zeller, M., Verwer, K., Eberli, G. P., Massaferro, J. L., Schwarz, E., & Spalletti, L. (2015). Depositional controls on mixed carbonate–siliciclastic cycles and sequences on gently inclined shelf profiles. *Sedimentology*, *62*(7), 2009–2037.

Zohdi, A., Mousavi-Harami, R., Moallemi, S. A., Mahboubi, A., & Immenhauser, A. (2013). Evolution, paleoecology and sequence architecture of an Eocene carbonate ramp, southeast Zagros Basin, Iran. *GeoArabia*, *18*(4), 49–80. https://doi.org/10.2113/geoarabia180449

Zuberi, A., & Dubois, E. P. (1962). Basin architecture, West Pakistan. *Pak-Stanvac Petroleum Project*, p11.

Zuchuat, V., Gugliotta, M., Poyatos-Moré, M., van Der Vegt, H., Collins, D. S., & Vaucher, R. (2023). Mixed depositional processes in coastal to shelf environments: Towards acknowledging their complexity. *The Depositional Record*, *9*(2), 206–212.

Zuffa, G. G. (1980). Hybrid Arenites: Their Composition and Classification. *Journal of Sedimentary Petrology*, *50*(1), 21–29. https://doi.org/10.1306/212F7950-2B24-11D7-8648000102C1865D